NASA CR-66344

THEORETICAL AND EXPERIMENTAL INVESTIGATION OF A THREE-DIMENSIONAL MAGNETIC-SUSPENSION BALANCE FOR DYNAMIC-STABILITY RESEARCH IN WIND TUNNELS

Status Report
1 March 1966 to 31 September 1966
1 October 1966 to 1 March 1967

National Aeronautics and Space Administration
Grant NGR 47-005-029

H. M. Parker
Principal Investigator
Ricardo Zapata and Robert Smoak

RESEARCH LABORATORIES FOR THE ENGINEERING SCIENCES
SCHOOL OF ENGINEERING AND APPLIED SCIENCE
UNIVERSITY OF VIRGINIA
CHARLOTTESVILLE, VIRGINIA

Report No. AST-4030-103-67U
April 1967

Copy No. _____

INTRODUCTION

The last semiannual status report (AST-4030-102-66U) was issued in March 1966. Since an extension with (small) additional funds to December 31, 1966 (from September 1, 1966) had been granted, it had been decided not to prepare a semiannual report covering the work from March 1, 1966 to September 31, 1966 but rather in the interest of efficiency to issue a final report. Recently, however, a proposal to NASA to continue and extend the research involved, including the development of a prototype cold magnetic balance and a demonstration of its feasibility, has been accepted in the form of an extension with (considerable) additional funds of the existing grant. Consequently, the present report may be considered as a status report covering two semiannual periods.

The following four sections summarize the work to date and provide a, hopefully, sound base on which the decisions relative to the prototype cold balance may be made. It should be noted that the important design decisions will result from a meeting of minds of the Langley Research Center and University of Virginia personnel involved in the project.

SECTION I
COIL CONFIGURATION DESIGN

The March 1966 semiannual status report presented some preliminary coil configuration designs and indicated the methods by which a reasonably optimum design, given performance and operating specifications, could be achieved. The reader is referred to the March 1966 status report for a discussion of the types of coil configurations ($\tan^{-1}\sqrt{2}$, $\tan^{-1}\sqrt{8}$, and $\tan^{-1}\sqrt{8}$ drag augmented systems) which are pertinent to balance design. Two types of calculations have been involved in the current studies.

First, for each of the coil types (e.g., $\tan^{-1}\sqrt{2}$ gradient coil, Z force coil, etc.) the basic calculation of field and/or field gradient at the symmetry point (sphere position) with a characteristic length in the geometry set equal to 1 cm has been extended to an adequately wide range of values of a parameter related to the size of the coil. The preliminary calculations had not covered a sufficiently wide range of coil sizes. Additionally, calculations were made for gradient and/or main field coils to fit in the space between the wind tunnel wall and the gradient coils (which had not been incorporated into the preliminary design. Of course, these results for a single absolute coil size (constant value for one characteristic length in the coil geometry) may be easily scaled to any absolute size for non-ferromagnetic cored coil configurations. The philosophy of designing for non-ferromagnetic cored systems is retained and thus leaves for future consideration (or as a factor of safety) the increase of performance to be realized by judicious use of ferromagnetic cores (Princeton experience indicates a gain of 2-3 is possible).

Secondly, and perhaps more importantly, these basic calculations have been used in systematic studies of the relationships between the various balance and performance parameters. Some of these relationships, especially those corresponding to constant relative geometry, can be rather easily predicted; others are not so apparent.

Figures 1-18 show plots of the field or the field gradient at the symmetry position for single coils of the various types. For each some characteristic length (defining an inner geometrical limit) is set to 1 cm. and the current density (uniform over the coil cross section) has been set to $J = 1000$ amps/cm^2. The scaling rules allow one to scale to different sizes and different current densities. The parameter A appearing in some of the figures is a parameter which determines the size of the coil (with a constant characteristic length). Specifically for gradient coils the outer boundary of the cross section is defined by

$$\rho = A(\sin 2\phi)^{1/3}$$

and A is, in units of the characteristic length, the maximum distance from the symmetry point (at $\phi = \pi$) of the contour for which at constant power maximum field gradient is produced (Gradient-Power contour). Similarly, for a field coil the outer boundary of the coil cross section is defined by

$$\rho = A(\sin\phi)^{1/2}$$

and A is, in units of the characteristic length, the maximum distance from the symmetry point (at $\phi = \pi/2$) of the contour for which at constant power maximum field is produced (Field-Power contour).

In both the $\tan^{-1}\sqrt{2}$ and $\tan^{-1}\sqrt{8}$ systems there is an annular space between the gradient coils and the tunnel wall and symmetrical about the symmetry plane in which either z force gradient coils or main field coils may be placed. For the $\tan^{-1}\sqrt{2}$ system the space if fairly large; for the $\tan^{-1}\sqrt{8}$ system the space is relatively small. Figures 3, 4, 5, 6 and 10, 11, 12, 13 (for $\tan^{-1}\sqrt{2}$ and $\tan^{-1}\sqrt{8}$ respectively) show gradients and fields (and volumes) of the symmetry plane coils on the basis that the most appropriate part of the space for gradient coils (on the appropriate side of the Gradient-Power contour) is used for gradient and the rest of the space is used for main field coils.

For the $\tan^{-1}\sqrt{2}$ system a use of this symmetry plane space for coils is a matter of total system decision since it prevents a direct, straight line observation of the model through the coil configuration in the symmetry plane. For the $\tan^{-1}\sqrt{8}$ system, the symmetry plane space, though much smaller, probably cannot be used for any other purpose.

It should be noted that the basic calculations represented by these eighteen figures allow easy, rapid calculations of specific coil configurations. Given the appropriate performance and operation specifications, a handy slide rule and 15 minutes of time can produce a corresponding coil configuration.

To effect a systematic study of parameter relationships, a program was written to calculate series of coil configurations. Input data were gradient coil, drag augmented gradient coil, and main field coil current densities (J_1, J_2, J_3), 3-D force to sphere weight ratio, drag augmented force to sphere weight ratio, the sphere density, and the wind tunnel radius. The magnetization of the sphere M was taken as $M = 3B/4\pi$, corresponding to high saturation magnetization material (e.g., iron), and the designs were calculated by stepping B from 1500 gauss to 15,000 gauss by increments of 500 gauss. The program calculated the various exclusion radii and scaled the coils appropriately. Two versions of the program were used for the $\tan^{-1}\sqrt{2}$ and $\tan^{-1}\sqrt{8}$ systems. The basic single coil calculations were made available to the program by a tabular interpolation method.

Calculations were made for all force to sphere weight ratios of 10, current densities ($J_1 = J_2 = J_3$) ranging from 500 amps/cm^2 to 10,000 amps/cm^2, and nominal tunnel radii ranging from 6 cm to 60 cm (tunnel diameters 4-3/4" to 4'). With the cold balance in mind, power and weight are calculated on the basis of Al at 20°K (resistivity of 1.7×10^{-9} ohm-cm and density of 2.7 gm/cm^3). While the studies have not been exhaustive, it is believed that the important trends have been found. It should be noted that from the calculations made in this way (specifically, M proportional to B) designs appropriate to a fixed M (effectively saturated M, e.g., a ferrite) can be extracted simply by looking at the results for an appropriate constant B. Since program difficulties limited

results for the case of symmetry plane space being used partly for Z force gradient coils and partly for main field coils, and since in the $\tan^{-1}\sqrt{8}$ system little can be gained by so splitting the use of the symmetry plane space, the $\tan^{-1}\sqrt{8}$ results used in the following summary correspond to the entire symmetry plane space being used for field coils.

A. As expected, from the earlier studies, the $\tan^{-1}\sqrt{2}$ system even with the use of the symmetry plane space is inferior in performance (by about 10% in power) to the $\tan^{-1}\sqrt{8}$ system. Thus, there seems to be no doubt that the $\tan^{-1}\sqrt{8}$ system ought to be used for the magnetic balance.

B. For the Iron Case (a term we shall use to designate the high saturated magnetization, M proportional to B operation) at constant tunnel radius and force capacity a minimum occurs in the total power vs. current density dependence (power minimized with respect to B, hence M at each current density). This minimum of B-optimized power occurs at a relatively low current density. Figure 19 shows the result for the 8 cm radius tunnel (tunnel diameter nominally 6.3" and a prime prospect for the prototype), and that the minimum occurs at about 1200 amps/cm^2. As the tunnel size increases the current density for minimum B-optimized power decreases somewhat. Figure 20, again for the 8 cm radius, shows total coil weight vs. current density for the B-optimized configuration. Inspection of figures 19 and 20 shows that a possible trade off between power and coil weight (hence bulk and size) exists. For example, going from $\sim$ 1200 amps/cm^2 to 2000 amps/cm^2 increases the power by about 12% and decreases the coil weight by a factor of 3. More dramatically, going from J$\cong$ 1200 amps/cm^2 to 7000 amps/cm^2 increases power by about 2 and decreases the coil weight by a factor of about 20. It is thus apparent that the current density at which the system may be operated has a very large influence on balance design.

C. For the Ferrite case (a term we shall use to designate the low saturated magnetization, hence fixed B mode of operation) at constant tunnel radius and force capacity, the total power vs. current density curve

exhibits a very flat minimum which shifts to lower current densities as the fixed B decreases. Figures 21 and 22 show total power and coil weight vs. current density for 8 cm radius and for (respectively) B = 1500 gauss and B = 2500 gauss (M ~ 360 gauss and 600 gauss). Of course, the power and weights are smaller in the latter case since the gradient required for a given force varies inversely with the sphere magnetization. Obviously, the feature of trading a little power for a large weight reduction by an increase in current density is, if anything, more prominent here.

D. An interesting comparison of the Iron and Ferrite cases is shown in figure 23 in which the log of the ratio of total Power at a variable tunnel radius to the power at a 6 cm radius taken as a reference is plotted against the logarithm of the ratio of the tunnel radius to 6 cm. For the Ferrite case B = 2500 gauss and J = 2000 amps/cm^2 and for the Iron case J= 2000 amps/cm^2 and the power is optimized with respect to B. The figure clearly shows the slower approach of the Iron Case to the large size limit of scaling as the cube of the scale factor. Moreover, it shows that at a four foot tunnel radius the B = 2500, J = 2000 Ferrite case is scaling (locally) as the cube of the scale.

The qualitative aspects of the above summary may be understood quite well from the scaling laws; the studies have served to quantify them. Probably of more importance the studies have focussed attention in a more quantitative way on two important, exceedingly important, aspects of magnetic balance design.

First, for the (engineeringly) rotationally free mode of operation (the Ferrite case) the value of the saturated magnetization attainable is of pertinent importance. One expects to find that, as the saturated magnetization of a sphere material increases, the losses and hence the torques due to rotation about an axis perpendicular to the main field will increase. Thus arises the very important question: How much balance damping can be tolerated? Effort in the area is already underway and the quite favorable but preliminary indication is that a material more lossy than the typical low-loss ferrite may be acceptable.

Second, the gain, especially in total coil weight at the larger sizes, to be achieved by operating at the higher densities indicates the great importance

of arranging efficient cooling. This aspect of the design interacts strongly with the capital investment and operating cost of the refrigeration system, as well as directly on the details of the coil configuration and support designs. As indicated in earlier reports, the present thought is to avoid a major effort in the area of cooling efficiency, but it is apparent that it may become a major concern in the mature stages of a successful cold magnetic balance development.

It should be noted that the design studies are continuing. One interesting and perhaps important idea which is being investigated is that of designing coils which carry varying currents for a higher current density than those which carry steady currents.

SECTION II
CONTROL SYSTEM

The control system and current source for the balance must meet several requirements. They must scale easily to the large powers required for a large tunnel. The closed loop response of the balance must be easily modified so that the characteristics of the balance may be tailored to the experiment in progress. This requires that the gradient coil current control system be fast enough that it will not be a barrier to achieving the desired overall balance performance.

All these requirements suggest a switched system for the current control. Scaling to large power will be less of a problem with a switched system. Since a fast control is required, a time optimal control law is the logical choice. This is the control law which reduces current error to zero in minimum time, i. e., using a bounded control, there is no other control law which will produce a faster response. For the current controls, the time optimal strategy is quite easy to understand. If it is desired to increase the current flowing in a coil one applies the maximum allowable voltage until the desired current is reached and then the appropriate voltage to maintain this current is applied. Using a time optimal current control will make it easier to construct a desired response for the entire balance. Should a time optimal control law be desired for the balance itself, having already constructed a time optimal current control as a subsystem will not be incompatible with the overall control.

The requirement for scaling to large power suggests the use of a controlled rectifier-inverter. Either silicon or mercury controlled rectifiers would be satisfactory. The SCR's appear to be the much better choice. They are more compact, faster, and handle high currents easily. The only real advantage of mercury rectifiers is that they recover from voltage breakdown while SCR's are destroyed.

If we consider one spatial dimension and the gradient coil associated with it , the system differential equations are:

$$m \frac{d^2x}{dt^2} = k\, i,$$

$$L \frac{di}{dt} = E(t).$$

$E(t)$ is the voltage applied to the gradient coil and k is the force per unit current. The resistance of the coil is negligible for the purposes of a dynamic analysis. The entire system can be represented schematically as shown in Diagram 1. A power source to drive current through a gradient coil in one direction is shown in Diagram 2. A similar network is required for currents in the opposite direction. This network is for a single phase power source. Multiple phase bridges are similar.

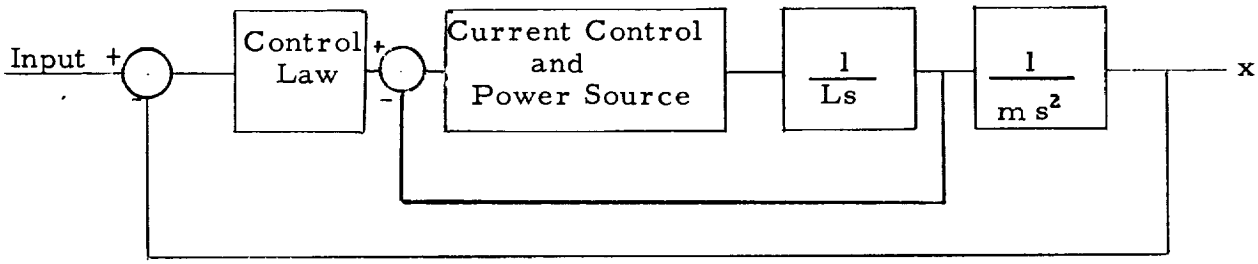

Diagram 1

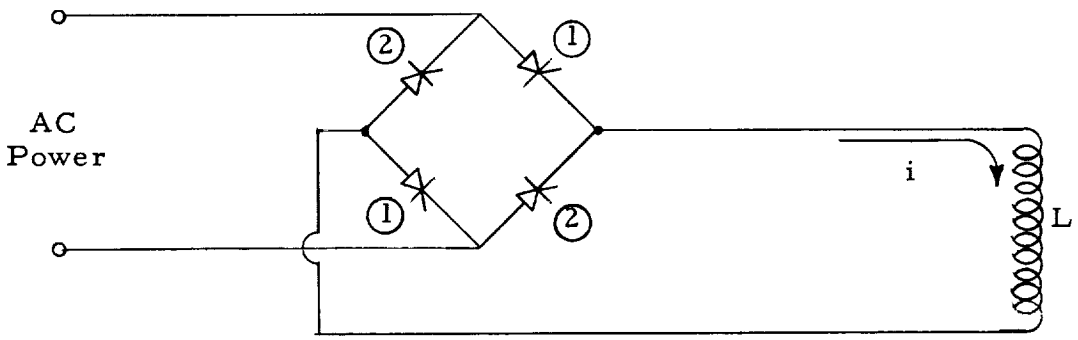

Diagram 2

To increase the current through L the diode pair (1) is fired during the entire positive half cycle of the AC source and the pair (2) is fired during the entire negative half cycle. To decrease the current through L while it is still flowing in the direction indicated we fire the pair (1) at the end of the positive half cycle and allow it to continue conducting almost to the end of the negative half cycle when pair (2) is fired shutting off pair (1) and then pair (2) conducts through the majority of the positive half cycle. In this mode the energy stored in L is being transferred back to the AC power source. Time average voltages between maximum and minimum can be achieved by varying the firing angle for the two arms of the bridge. The response of such a bridge is limited by the time for 1/2 cycle of AC power, the speed of the triggering circuitry, and the physical properties of the rectifiers. The techniques involved in constructing such a device are well within the current state of the art.

If the frequencies of interest in the control system are small with respect to the frequency of the AC power source, the displacement response to the undesirable signal (AC component) will be negligible. If this AC frequency is 5 times the highest system frequency, the AC response will be approximately 10^{-3} times the desired response. The frequency of the undesired signal can be raised by using a 3 or 6 phase system. The use of more phases also greatly reduces the amplitude of the undesired signal and gives some improvement in the frequency response of the power source. If a basic (input) AC frequency of 60 cps is too low,

a motor generator set can easily supply the required AC power at a higher frequency. Or a combination solid state frequency multiplier and current control might be more economical.

The system described above uses the AC source to turn off the SCR's. Another possibility under consideration is the use of SCR's to switch power from two DC sources. In this approach the turning off of the SCR's can be accomplished much more quickly. The disadvantage of this approach is that additional circuitry must be employed to turn off the SCR's. Fewer SCR's will be required to handle large powers so this approach may turn out to be superior. The choice of power source is very closely tied to the required frequency response of the balance.

In order to achieve a stable motion near the origin, i.e., when the current is at its desired value, the bang-bang or switch will be replaced by a saturable linear gain. Thus the control function

$E = \operatorname{sgn} x$ will be replaced by $E = (\operatorname{sgn} x)(\min(|ax|, 1))$, where

a is the linear gain, and x is the desired current minus the actual current.

If a switched control is used for the displacement coordinates, a similar scheme will be used. The result will be that for large disturbances, the system will have essentially an optimal control law and there will be a linear mode for small disturbances near the desired state.

The calculations to date have found the coil shapes but have not specified the number of turns and thus the inductance and resistance. It is easily shown that the response time for current (and thus force) in a coil is proportional to the number of turns in the coil and the desired force change to be accomplished while it is inversely proportional to the exitation voltage. Thus, from a control point of view, coils with a small number of turns will be more satisfactory. The exitation voltage is limited in the voltage ratings in SCR's. A value of 400 volts leaves a reasonable safety factor here.

SECTION III
DESIGN OF LOW TEMPERATURE MAGNETS

A survey of the state-of-the-art in cryogenic magnet technology has been completed. From this several guidelines for the design of the magnet system were obtained.

A. General Coil Type:

Since high current densities are desired and simplicity of design and operation are important, the choice is reduced to supercooled and superconducting magnets. It is felt at this time that a hybrid system consisting of superconducting DC magnets (field coils and drag augmentation coils) and AC supercooled magnets (gradient coils) should offer an attractive combination of desirable features. Superconductors result in minimum expenditure of coolant, although their use restricts the choice of operating temperature to that of liquid helium. Not enough is known at present about AC performance of superconducting magnets. It is quite probable that for AC operation complete stabilization would be required and losses would be those corresponding to the stabilizing material. Thus it makes more sense to approach the problem with an optimum design of low resistivity coils. Furthermore, it is felt quite strongly that in a prototype system as this it will be beneficial to acquire experience with both types of magnets, particularly since this application to magnetic wind tunnel balances poses several new technological questions that will only find satisfactory answers in the laboratory.

B. Coil Material:

For supercooled coils, aluminum of high purity (99.99% or higher) offers the best combination of low resistivity in the presence of magnetic fields, low specific weight and moderate cost. Experience of other workers in the field suggests that large cross sectional area results in more efficient cooling allowing higher packing fractions. Large cross sections will also result in lower inductance, a desirable feature for fast modulation of the coil current.

For the superconducting coils there is a wide choice of materials because the maximum magnetic fields will be quite moderate (10-20 kilogauss). It is anticipated that the price will be the deciding factor in this case.

C. Cryogenic Considerations:

For the sake of simplicity of design it appears desirable to have all magnets in a common dewar. This means a single coolant operating at or around liquid helium temperature. Recent publications in the field of superconducting magnet cooling clearly point out that utilization of liquid helium latent heat of vaporization represents only a lower limit in heat transfer capability in the 4°K temperature range. Appropriate design of return passages for the helium vapors can significantly decrease the rate of helium evaporation, particularly around the current leads. Supercritical helium (4.2°K, 100 atm.) has very recently been proposed as an ideal heat transfer medium. This problem is presently receiving considerable attention from us since lower coolant consumption represents increased testing time and lower operating cost.

D. Current Density Levels:

An important design parameter is the maximum current density tolerated by the windings on a steady state basis. In fact this parameter will determine the all important question of coil size for specified magnetic field intensities and gradients. A summary of figures quoted by different workers in the field is given in Table 1. Effective current density is obtained by multiplying the value quoted for the conductor by the coil packing fraction λ. It is interesting to note that the value of λ is about 0.5 for magnets cooled by boiling heat transfer. The magnet reported by the Boulder group was cooled by forced connection with a gain in λ of about a factor of 2.

Table 1

Group	Coolant	Coil Material	λ	J_{max}, A/cm^2
NASA Lewis	Liq. Neon	99.998% Al	0.40	6.0×10^3
N.B.S. Boulder	Liq. Hydrogen	99.998% Al	.90	9.0×10^3
U. Cal. Los Alamos	Liq. Hydrogen	Pure Copper	.48	1.0×10^4
CRTBT Grenoble	Liq. Nitrogen	Copper	.46	2.7×10^3
GDL Princeton	Water	Copper	.62	5.6×10^2

A representative value for superconducting coils is 10^4 A/cm^2. It should be noted that the quoted figures for current density of cryogenic magnets are substantially higher than the value 10^3 A/cm^2 assumed for both water cooled copper and $20^{\circ}K$ aluminum coils in the sample calculation presented in the last progress report. Thus a considerable saving of conductor weight and consequently, of required coolant can be effected and even greater flexibility in the choice of power level and conductor size is possible.

SECTION IV
STABILITY ANALYSIS APPLICATION

Since it is a goal of the cold balance prototype program to demonstrate the feasibility of the 3-D magnetic balance method of investigating dynamic stability, indeed since this application is perhaps the most important potential, it is pertinent to the program to make a serious and detailed analysis of how it is to be done, including best possible estimates of the accuracy which may be attainable. Effort in this area is already underway, and the purpose of this section is to report the (relatively few) initial conclusions.

The initial work has been rather fundamental in character and has proceeded along the following lines. The three dimensional motion of a rigid body subjected to varying external moments is a complicated problem. Fortunately the problem involved here, the inverse problem corresponding to "given the motion, what are the moments," is in principle considerably simpler than the direct problem, "given the moments, what is the motion." In the direct problem one is faced with the necessity of solving a complicated set of (in some cases at least importantly nonlinear) differential equations. In the inverse problem, ideally the body characteristics and the motion as a function of time are known and the describing equations reduce to a set of algebraic equations for the forces and moments. Of course, when the dependence of the forces and moments on the motion variables becomes complicated the problems of solution and interpretation are not trivial.

In the usual formulation of the equations of motion of a rigid body of fixed mass distribution, the motion of the body is described in terms of a translational motion of a reference point fixed in the body and a rotation of the rigid body about that reference point. The translational equation of motion reduces to the simple form

$$\vec{F}_{ext} = m \frac{d^2 \vec{r}_c}{dt^2}$$

where the left member is the sum of the external forces acting on the body, m is the mass of the rigid body, $\vec{r}'_c$ is the position vector of the center of mass of the rigid body referred to an inertial reference frame from which the observations are made. In other words, this simple form results when the reference point fixed in the body (used in describing the motion) is chosen to be the center of mass; with any other choice ($\vec{r}'_c$ the position vector of a reference point other than the center of mass) an additional term appears in the translational equation of motion.

In a similar fashion, the rotational equation of motion reduces to

$$\vec{M}_{ext} = \frac{d\vec{L}}{dt} \; : \; \vec{L} = \Sigma \, m_i \vec{\rho}_i \times (\vec{\omega} \times \vec{\rho}_i)$$

where $\vec{M}_{ext}$ is the sum of the moments of the external forces about the reference point, $\vec{L}$ is the total angular momentum of the system about the reference point as observed from the inertial reference frame, and the reference point is either (a) a point in the body fixed in the inertial reference frame (rotation about a fixed point) or (b) the center of mass of the body. Again if the reference point satisfies neither of these two conditions, the rotational equation of motion contains additional terms.

In the most general mode of operation of the 3-D magnetic balance, the magnetic sphere embedded in a non-magnetic model will not be at the center of mass of the model and the sphere center will not be a fixed point (e.g., the sphere center can be oscillated laterally in an attempt to disentangle $C_{m_{\dot{\alpha}}}$ and C_{m_q}). Since the balance control system involves a subsystem to sense the position of the sphere center, one expects the directly observed motion to be the translational motion of the sphere center and the rotational motion about the sphere center. Thus the question arises as to whether it is more convenient to choose the center of mass as the reference point and therefore have the simpler equations of motion and to transfer the observed motion to the center of mass, or to use the sphere center as the reference point accepting the more complicated equations of motion but having the observed motion apply directly.

At the outset, two generalities may be stated. First, from the point of view of describing the motion by using a fixed inertial reference frame and a second reference frame (in general) translating and rotating with respect to the fixed frame, it is obviously more convenient to choose the moving frame in such a way that the moment of inertia tensor of the body, referred to the moving frame, has constant elements. [Time varying inertial parameter is too much!] For the non-axially symmetrical body this means fixing the moving frame to the body. For the effectively axially-symmetrical body a single degree of freedom of body with respect to moving frame is permissible, even convenient, e.g., the non-rolling aeroballistic moving frame used for missile configurations.

Secondly, it is easy to show (either intuitively or analytically) that in describing the general motion, translation and rotation, of a rigid body using a fixed inertial frame and a moving frame fixed in the body, the angular velocity that results is, for a given motion of the body, independent of the choice of the reference point (i.e., the point in the body chosen as the origin of the moving frame). Thus, for our problem, the angular velocity about the sphere center is the same as the angular velocity about the center of mass, and the angular velocity transfers directly.

To develop the general case for the application considered here, let us assume or define the following:

$o'x'y'z'$ - a fixed, inertial reference frame

$s\ x\ y\ z$ - a moving frame attached to the body (the origin S is to be the position of the center of the magnetic sphere)

$\vec{r}'_s, \vec{r}'_c, \vec{r}'_i$ - position vectors referred to the inertial frame $x'y'z'$ of respectively, the point S, the center of mass of the body C, and a mass element m, of the body

$\vec{\rho}_i$ - the position vector of m_i with respect to the mass center C

$\vec{\eta}_i$ - the position vector of m_i with respect of the sphere center S

$\vec{\rho}_s$ - the position vector of S with respect to the mass center C($-\vec{\rho}_s$ is the position vector of C with respect to S).

Then $\Sigma\, m_i \vec{\rho}_i = 0$ and $\Sigma\, m_i \vec{\eta}_i = -m\vec{\rho}_s$ where the sums are taken over all the mass elements of the body, m is the total mass of the body, and the minus sign in the second equation appears because of the way $\vec{\rho}_s$ is defined. Further

$$\vec{\eta}_i = \vec{\rho}_i - \vec{\rho}_s$$

$$\vec{r}'_i = \vec{r}'_c + \vec{\rho}_i \quad \text{and} \quad \vec{r}'_i = \vec{r}'_s + \vec{\eta}_i$$

follow from the definitions. Since $\vec{\eta}_i$, $\vec{\rho}_i$, and $\vec{\rho}_s$ are referred to the moving frame (written in terms of components in the xyz frame) one can derive the usual expression

$$\frac{d}{dt} = \frac{\delta}{\delta t} + \vec{\omega} x$$

where $\vec{\omega}$ (also expressed in terms of components in the xyz frame) is the angular velocity of the moving frame and $\delta/\delta t$ is the time rate of change as observed by an observer fixed in (and rotating with) the moving frame, e. g., for

$$\vec{\rho}_i = x_i\, i + y_i j + z_i k \quad (i, j, k \text{ unit vectors in } x,\ y,\ z)$$

then

$$\frac{\delta \vec{\rho}_i}{\delta t} = \frac{dx_i}{dt} i + \frac{dy_i}{dt} j + \frac{dz_i}{dt} k.$$

Writing Newton's second law for the i^{th} mass element

$$\vec{F}_i = m_i \frac{d^2 \vec{r}'_i}{dt^2},$$

summing over the body, noting that the internal forces disappear,

$$\vec{F}_{ext} = \Sigma \vec{F}_i = \Sigma\, m_i \frac{d^2\vec{r}'_i}{dt^2}$$

and replacing $\vec{r}'_i$ by $\vec{r}'_s + \vec{\eta}_i$, one gets

$$\vec{F}_{ext} = \Sigma\, m_i \left(\frac{d^2\vec{r}'_s}{dt^2} + \frac{d^2\vec{\eta}_i}{dt^2}\right) = m \frac{d^2\vec{r}'_s}{dt^2} + \frac{d^2}{dt^2}\left(\Sigma\, m_i \vec{\eta}_i\right)$$

$$\vec{F}_{ext} = m \frac{d^2\vec{r}'_s}{dt^2} - m \frac{d^2\vec{\rho}_s}{dt^2} \quad .$$

This translational equation could have been derived from the usual result (when the reference point is chosen to be the center of mass) by noting that $\vec{r}'_c = \vec{r}'_s - \vec{\rho}_s$. Thus it corresponds directly to the usual theorem concerning the motion of the center of mass of a system. Here, however, with the reference point not the center of mass the additional term appears unless $d^2\vec{\rho}_s / dt^2$ is zero.

To develop the rotational equation of motion one must look at the angular momentum. By definition the angular momentum about c, the mass center is

$$\vec{L}_c = \Sigma\, m_i \vec{\rho}_i \times \frac{d\vec{r}'_i}{dt} = \Sigma\, m_i \vec{\rho}_i \times \left(\frac{d\vec{r}'_c}{dt} + \frac{d\vec{\rho}_i}{dt}\right).$$

For our case, the body is rigid, the moving frame xyz is fixed to the body so that the $\delta / \delta t$ portions of the time derivatives of $\vec{\rho}_i$, $\vec{\rho}_s$ and $\vec{\eta}_i$ are zero giving

$$\frac{d\vec{\rho}_i}{dt} = \vec{\omega} \times \vec{\rho}_i, \quad \frac{d\vec{\rho}_s}{dt} = \vec{\omega} \times \vec{\rho}_s, \quad \text{and} \quad \frac{d\vec{\eta}_i}{dt} = \vec{\omega} \times \vec{\eta}_i.$$

Thus,

$$\vec{L}_c = \Sigma\, m_i \vec{\rho}_i \times (\vec{\omega} \times \vec{\rho}_i) + (\Sigma\, m_i \vec{\rho}_i) \times \frac{d\vec{r}'_c}{dt}$$

or

$$\vec{L}_c = \Sigma\, m_i \vec{\rho}_i \times (\vec{\omega} \times \vec{\rho}_i),$$

the usual expression for the angular momentum about the mass center. By definition, the angular momentum about S is

$$\vec{L}_s = \Sigma\, m_i \vec{\eta}_i \times \frac{d\vec{r}'_i}{dt}.$$

Rearranging as follows,

$$\vec{L}_s = \Sigma\, m_i (\vec{\rho}_i - \vec{\rho}_s) \times \left(\frac{d\vec{r}'_c}{dt} + \frac{d\vec{\rho}_i}{dt} \right)$$

$$= (\Sigma\, m_i \vec{\rho}_i) \times \frac{d\vec{r}'_c}{dt} + \Sigma m_i \vec{\rho}_i \times (\vec{\omega} \times \vec{\rho}_i) - (\Sigma m_i) \vec{\rho}_s \times \frac{d\vec{r}'_c}{dt} - \vec{\rho}_s \times \frac{d}{dt}(\Sigma m_i \vec{\rho}_i)$$

$$= \Sigma\, m_i \vec{\rho}_i \times (\vec{\omega} \times \vec{\rho}_i) - \vec{\rho}_s \times \left(m \frac{d\vec{r}'_c}{dt} \right)$$

one sees that

ang. mom. about S = ang. mom. about C + moment of linear moment of c. m. about S.

Rearranging differently,

$$\vec{L}_s = \Sigma\, m_i \vec{\eta}_i \times \left(\frac{d\vec{r}'_s}{dt} + \frac{d\vec{\eta}_i}{dt} \right)$$

$$= \Sigma\, m_i \vec{\eta}_i \times (\vec{\omega} \times \vec{\eta}_i) + \Sigma\, m_i \vec{\eta}_i \times \frac{d\vec{r}'_s}{dt}$$

$$\vec{L}_s = \Sigma\, m_i \vec{\eta}_i \times (\vec{\omega} \times \vec{\eta}_i) - m\vec{\rho}_s \times \frac{d\vec{r}'_s}{dt}$$

Note that in this case that the quantity $\Sigma\, m_i \vec{\eta}_i \times (\vec{\omega} \times \vec{\eta}_i)$ is not the angular momentum about S unless $\vec{\rho}_s \times d\vec{r}'_s/dt$ is zero (i.e., unless $\vec{\rho}_s = 0$, $d\vec{r}'_s/dt = 0$, or $\vec{\rho}_s$ and $d\vec{r}'_s/dt$ are parallel). Nevertheless, it is the quantity which is analogous to the usual expression for the angular momentum about the mass center and may be written in terms of moments and products of inertia about S and the components of the angular velocity.

The rotational equations of motion may be attained by differentiating the original expression for the angular momentum about S:

$$\frac{d\vec{L}_s}{dt} = \Sigma\, m_i \frac{d\vec{\eta}_i}{dt} \times \frac{d\vec{r}'_i}{dt} + \Sigma\, m_i \vec{\eta}_i \times \frac{d^2\vec{r}'_i}{dt^2} \quad .$$

From the second law $m_i \dfrac{d^2\vec{r}'_i}{dt^2} = \vec{F}_i$ and if one assumes (as usual) the colinearity of the 3rd law pair internal forces, the last term reduces to the moment of the external force about S.

$$\frac{d\vec{L}_s}{dt} = \Sigma\, m_i \frac{d\vec{\eta}_i}{dt} \times \left(\frac{d\vec{r}'_s}{dt} + \frac{d\vec{\eta}_i}{dt} \right) + \vec{M}_{ext}$$

$$= - \frac{m d\vec{\rho}_s}{dt} \times \frac{d\vec{r}'_s}{dt} + \vec{M}_{ext}$$

or

$$\vec{M}_{ext} = \frac{d\vec{L}_s}{dt} + \frac{m d\vec{\rho}_s}{dt} \times \frac{d\vec{r}'_s}{dt} .$$

Substituting for $\vec{L}_s$ from the above, one gets

$$\vec{M}_{ext} = \frac{d}{dt}[\Sigma\, m_i \vec{\eta}_i \times (\vec{\omega} \times \vec{\eta}_i)] - m \frac{d}{dt}[\vec{\rho}_s \times \frac{d\vec{r}'_s}{dt}] + m \frac{d\vec{\rho}_s}{dt} \times \frac{d\vec{r}'_s}{dt}$$

$$\vec{M}_{ext} = \frac{d}{dt}[\Sigma\, m_i \vec{\eta}_i \times (\vec{\omega} \times \vec{\eta}_i)] - m \vec{\rho}_s \times \frac{d^2\vec{r}'_s}{dt^2} .$$

In summary then, if the center of mass is chosen as the reference point, the equations of motion are

I. Translational $\qquad \vec{F}_{ext} = m \frac{d^2\vec{r}'_c}{dt^2}$

II. Rotational $\qquad \vec{M}_{ext} = \frac{d}{dt} [\Sigma\, m_i \vec{\rho}_i \times (\vec{\omega} \times \vec{\rho}_i)] .$

If the sphere center S is chosen to be the reference point, then the equations of motion are

III. Translational $\qquad \vec{F}_{ext} = m \frac{d^2\vec{r}'_s}{dt} - m \frac{d^2\vec{\rho}_s}{dt^2}$

IV. Rotational $\qquad \vec{M}_{ext} = \frac{d}{dt} [\Sigma\, m_i \vec{\eta}_i \times (\vec{\omega} \times \vec{\eta}_i)] - m\vec{\rho}_s \times \frac{d^2\vec{r}'_s}{dt^2} .$

In both cases the sum of the external forces, $\vec{F}_{ext}$, includes the aerodynamic forces, the gravitational forces, and the balance forces (acting at the sphere center). In the mass center case (I and II) $\vec{M}_{ext}$ includes the aerodynamic moments about c and the moments about c of the balance forces.

In the sphere center case (III and IV) $\vec{M}_{ext}$ includes aerodynamic moments about S (in general somewhat different from those about c) and the moment about S of the weight of the model, but does not, ideally, include any moments due to the balance. The right sides of the two translational equations require for this evaluation precisely the same input data, the acceleration of the mass center. The right sides of equations II and IV are significantly different. The right side of II requires the inertial parameters about c and the component of $\vec{\omega}$ and $\dot{\vec{\omega}}$; for IV one requires the inertial parameter about S, the components of $\vec{\omega}$ and $\dot{\vec{\omega}}$, $\vec{\rho}_s$, and the acceleration of S.

Thus, from the point of view of reducing data to attain information about the aerodynamic forces and moments, it appears that (1) the translational equations for the cases involve identical processes, and (2) the rotational equations involve different processes which may or may not be practically significant. In the mass center case (II), $\vec{\rho}_s$ and the balance forces must be used to find the balance moments about c. In the sphere center case (IV) $\vec{\rho}_s$ and the model weight must be used to find the moment of the weight about S and $\vec{\rho}_s$ and the acceleration of S must be used on the right side. One could suspect that the accuracy to be obtained might be related to the magnitudes of the various terms. Indeed, one could speculate that it is desirable to use both approaches for a confident reduction of data.

GUIDE TO FIGURES

Figures 1 through 18

Correspond to single coils of type indicated

Current density is 1000 amps/cm^2

Field in units of gauss

Gradient in units of gauss/cm

Volume in units of cm^3

Characteristic length, which is set equal to 1 cm, is

a) tunnel radius for $\tan^{-1}\sqrt{2}$ and $\tan^{-1}\sqrt{8}$ gradient coils and symmetry plane coils

b) gradient coil ($\tan^{-1}\sqrt{2}$ or $\tan^{-1}\sqrt{8}$) exclusion radius for Z-force coil

c) Z-force exclusion radius for main field coils

Inner boundary of main field coil section is circular about symmetry point

Figures 19 through 23

Correspond to entire drag augmented $\tan^{-1}\sqrt{8}$ system

All force capacity to sphere weight ratios are 10

Iron sphere is assumed

Figures 19 and 20: at each current density total power is minimized with respect to the main field B. ($M = \frac{3B}{4\pi}$.) Tunnel radius is 8 cm

Figures 21 and 22: Constant B (1500 and 2500 gauss), corresponds to ferrite case, tunnel radius is 8 cm

Figure 23: Total power vs. size, non-dimensionalized, for Iron case and a ferrite case

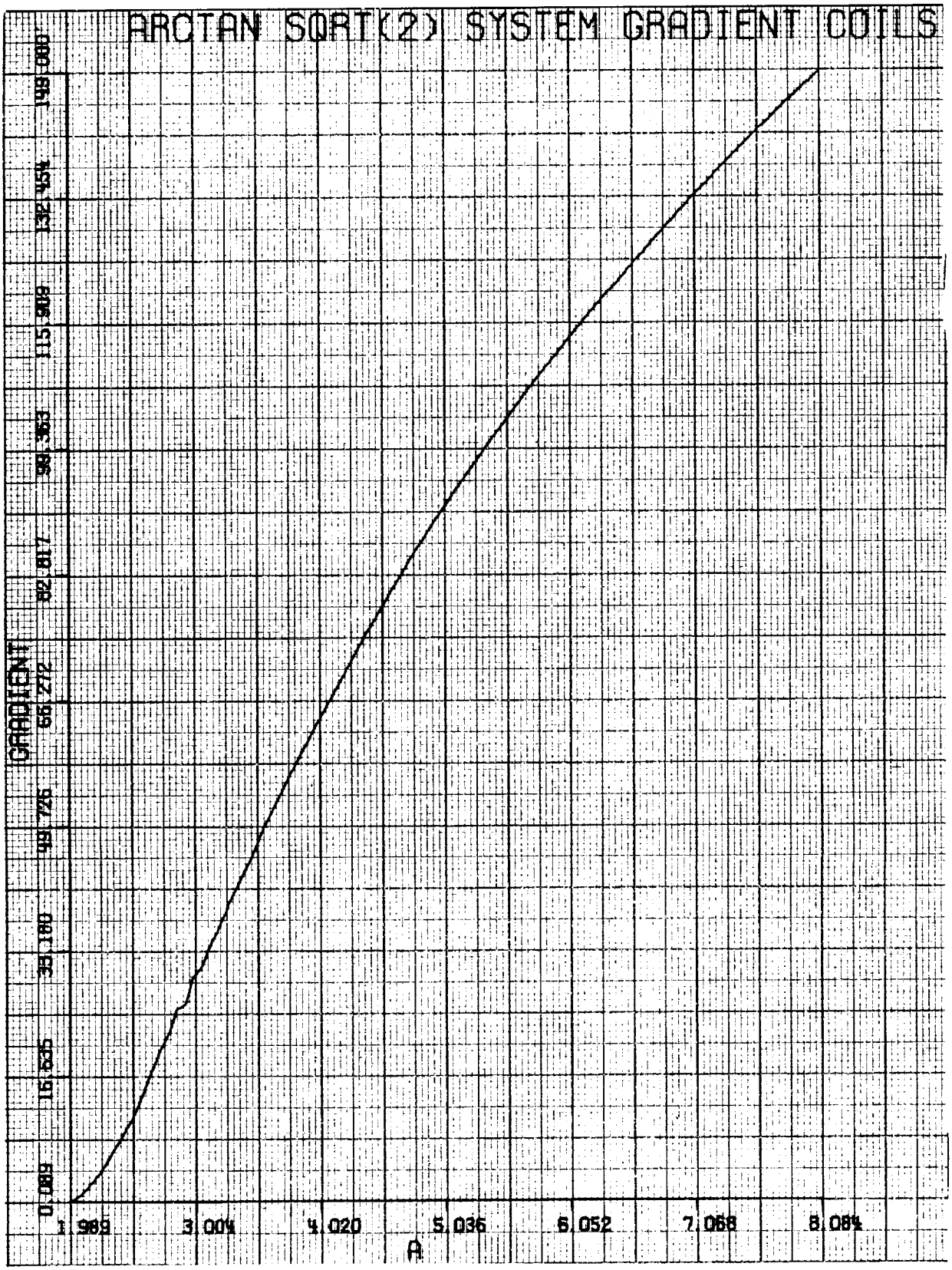
ARCTAN SQRT(2) SYSTEM GRADIENT COILS
GRADIENT
0.089
16.635
33.180
49.726
66.272
82.817
98.363
115.909
132.454
149.000
1.989
3.004
4.020
5.036
6.052
7.068
8.084
A

FIGURE 1

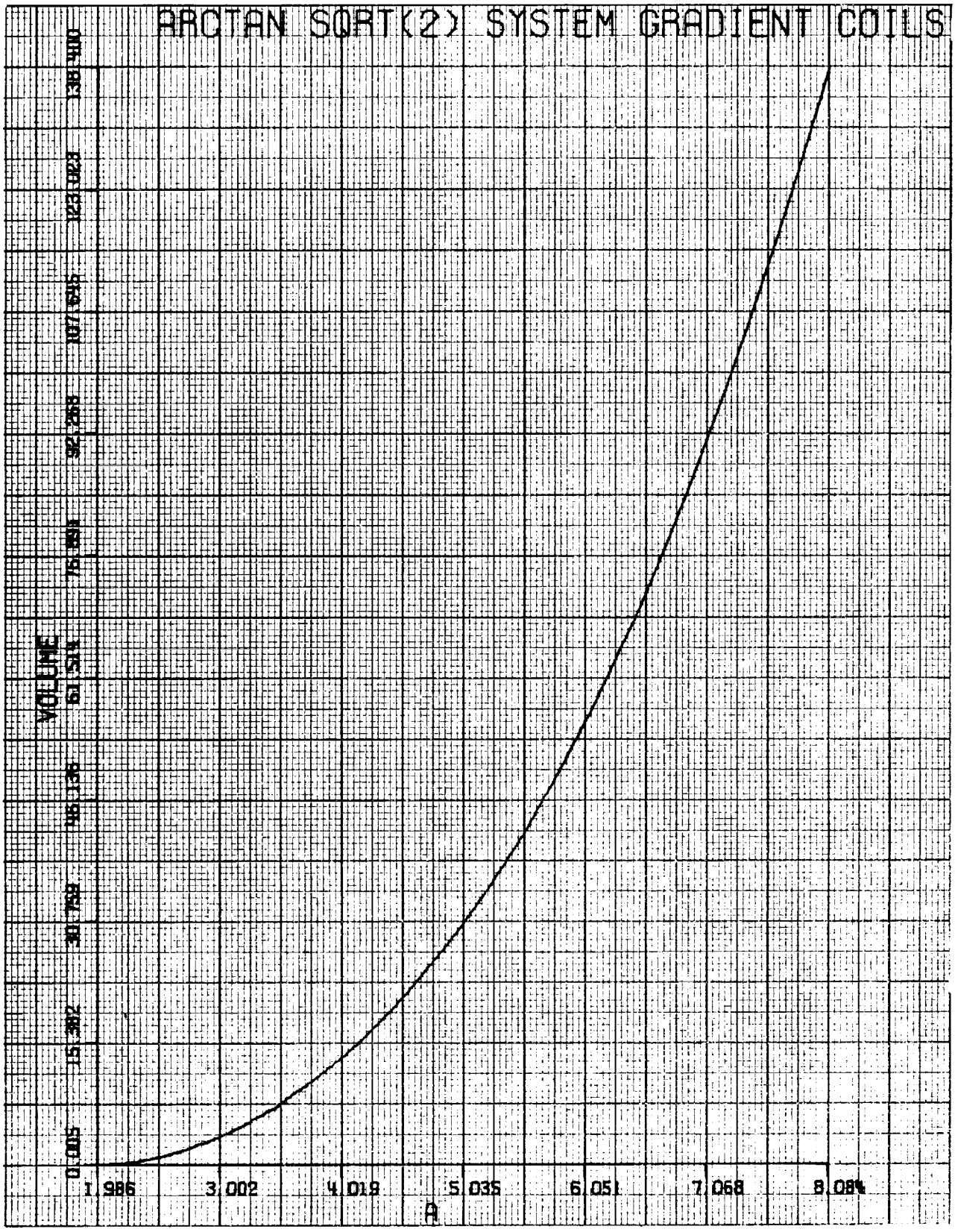
ARCTAN SQRT(2) SYSTEM GRADIENT COILS
VOLUME
0.005
15.382
30.759
46.136
61.513
76.890
92.268
107.645
123.023
138.400
1.986
3.002
4.019
5.035
6.051
7.068
8.084
A

FIGURE 2

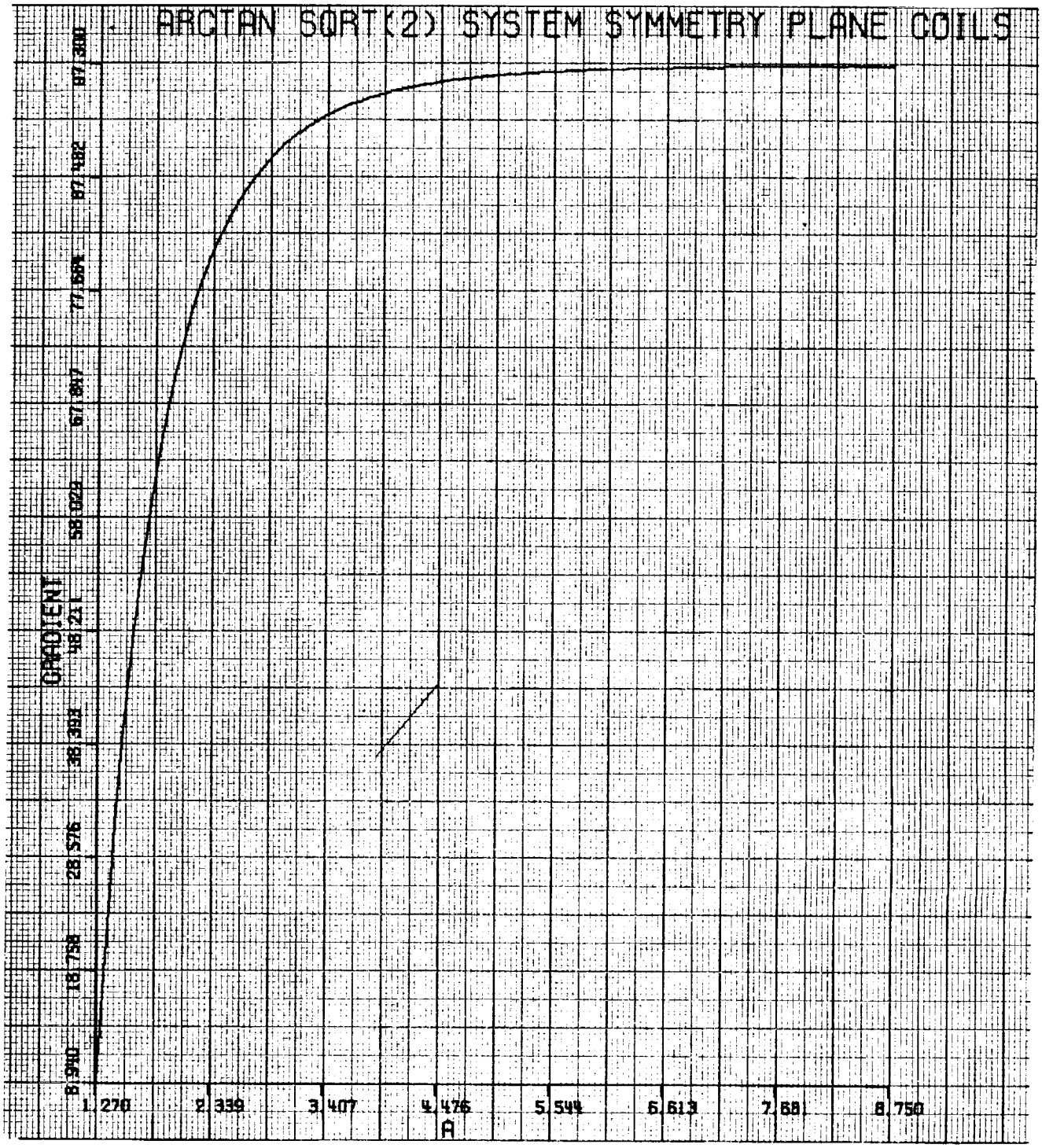
ARCTAN SQRT(2) SYSTEM SYMMETRY PLANE COILS
GRADIENT
97.380
87.482
77.585
67.687
57.790
48.211
38.393
28.576
18.758
8.940
1.270
2.339
3.407
4.476
5.544
6.613
7.681
8.750
A

FIGURE 3

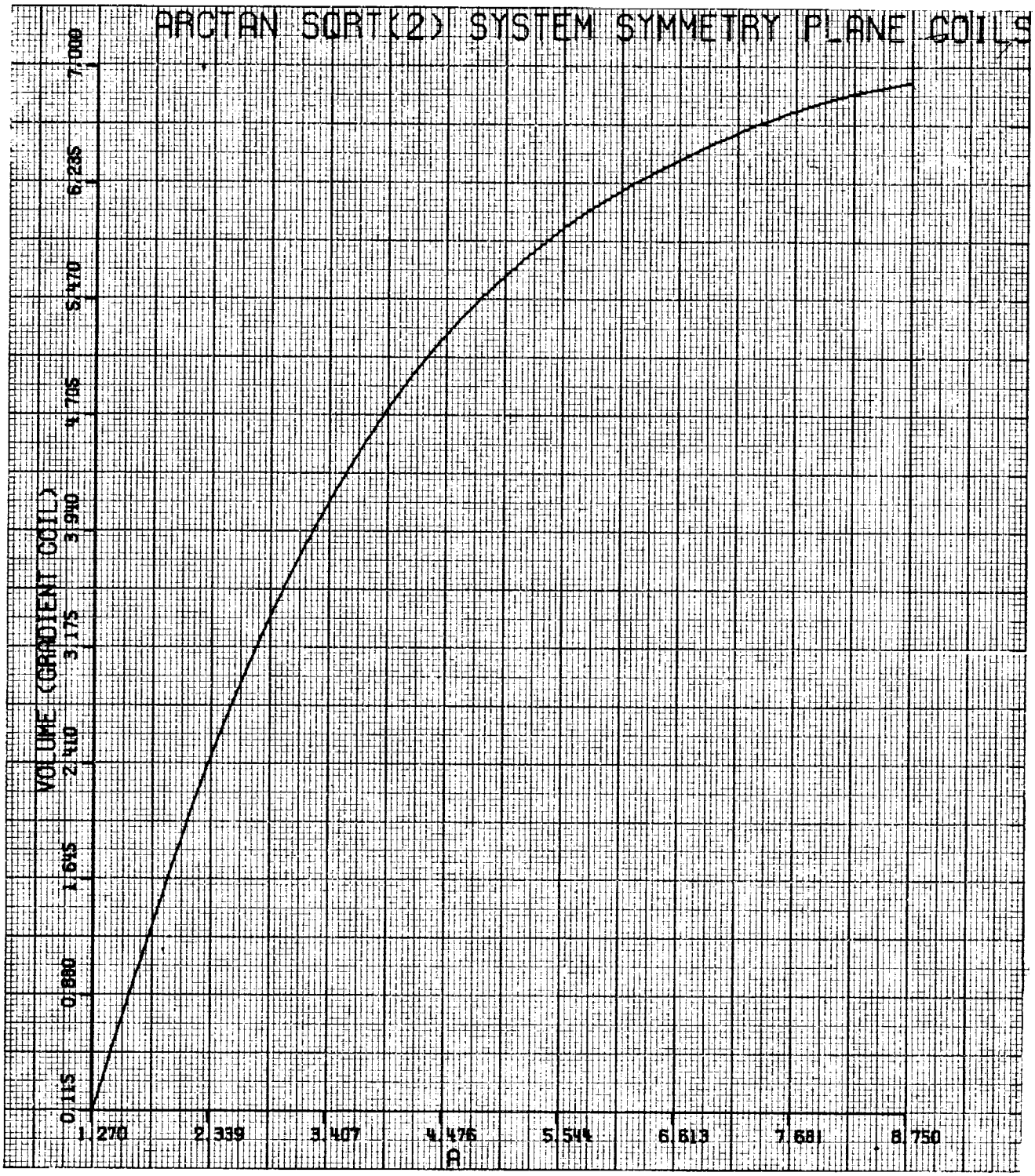
ARCTAN SQRT(2) SYSTEM SYMMETRY PLANE COILS
VOLUME (GRADIENT COIL)
0.115
0.880
1.645
2.410
3.175
3.940
4.705
5.470
6.235
7.000
1.270
2.339
3.407
4.476
5.544
6.613
7.681
8.750
A

FIGURE 4

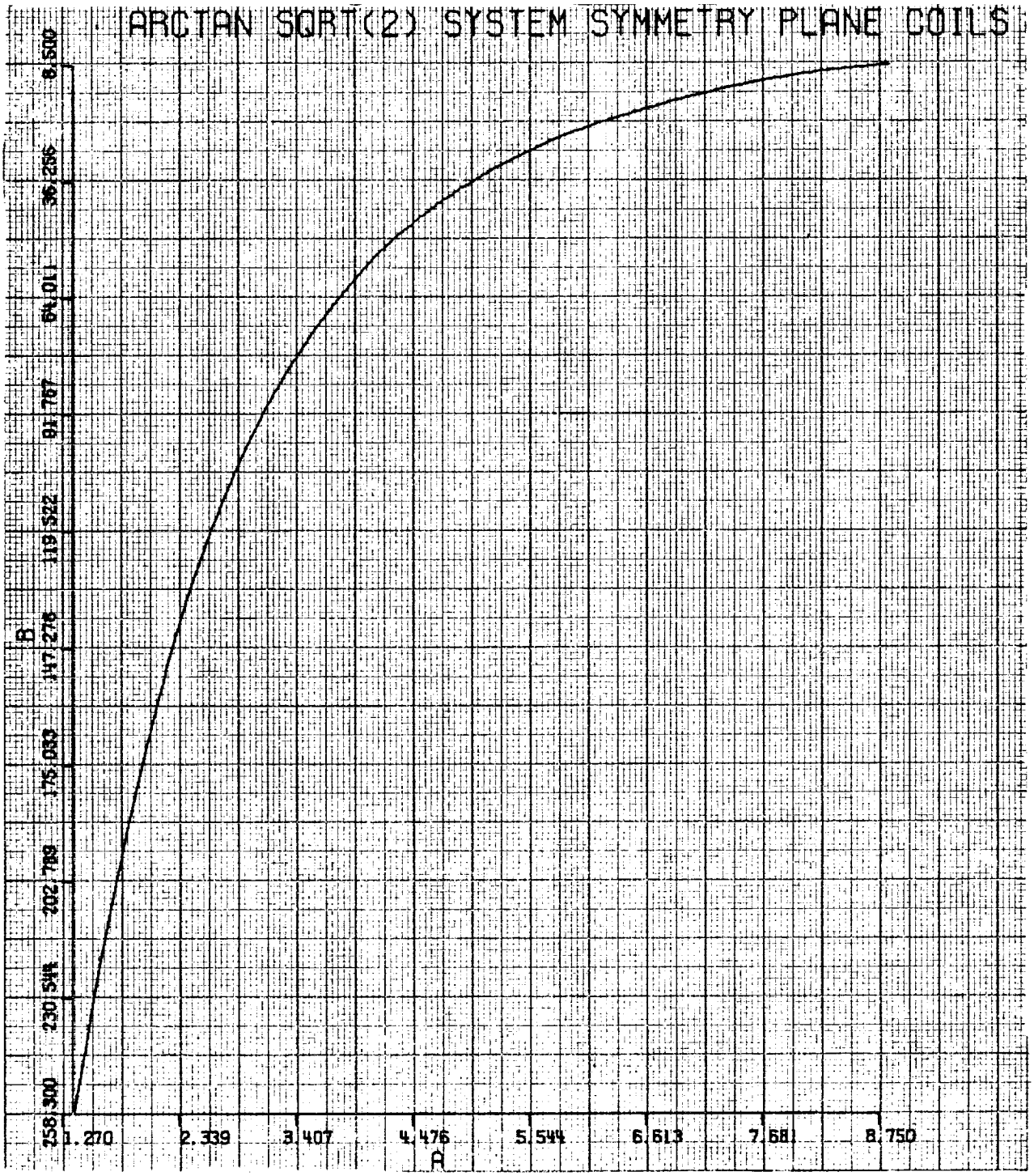
ARCTAN SQRT(2) SYSTEM SYMMETRY PLANE COILS
B
8.500
36.256
64.011
91.767
119.522
147.278
175.033
202.789
230.544
258.300
1.270
2.339
3.407
4.476
5.544
6.613
7.681
8.750
A

FIGURE 5

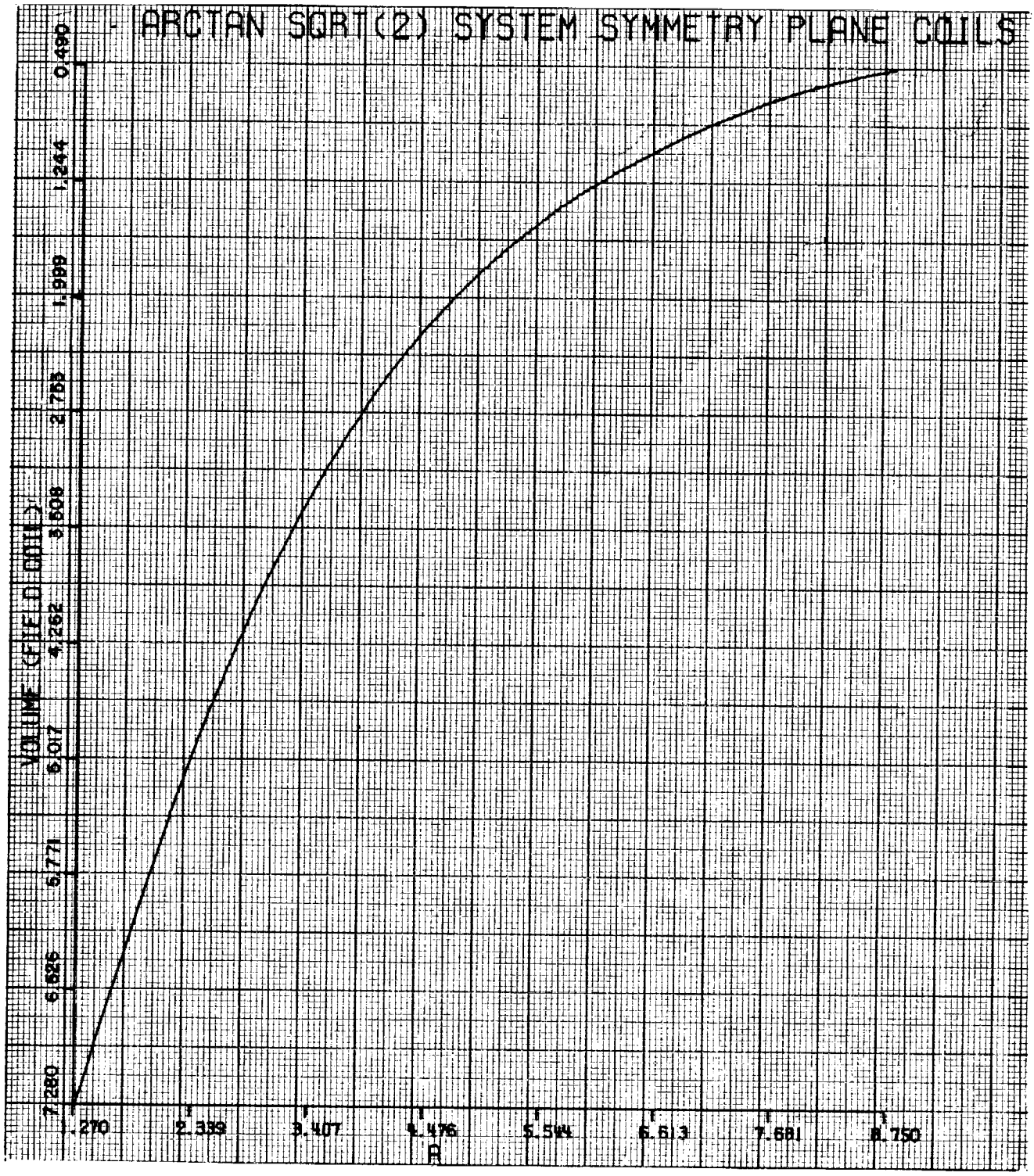
ARCTAN SQRT(2) SYSTEM SYMMETRY PLANE COILS
VOLUME (FIELD COILS)
0.490
1.244
1.999
2.753
3.508
4.262
5.017
5.771
6.525
7.280
1.270
2.339
3.407
4.476
5.544
6.613
7.681
8.750
R

FIGURE 6

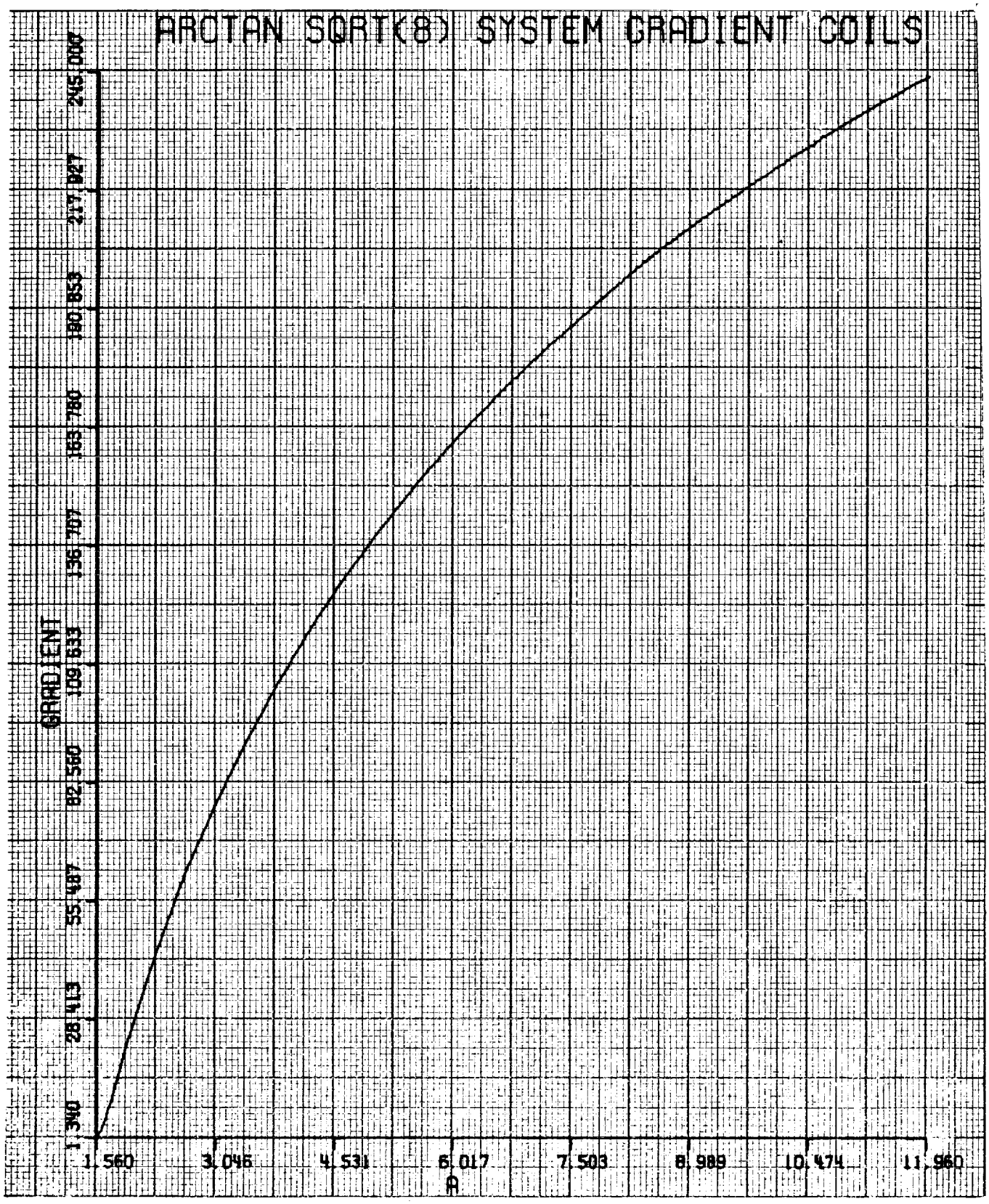
ARCTAN SQRT(8) SYSTEM GRADIENT COILS
GRADIENT
245.000
217.927
190.853
163.780
136.707
109.633
82.560
55.487
28.413
1.340
1.560
3.046
4.531
6.017
7.503
8.989
10.474
11.960
A

FIGURE 7

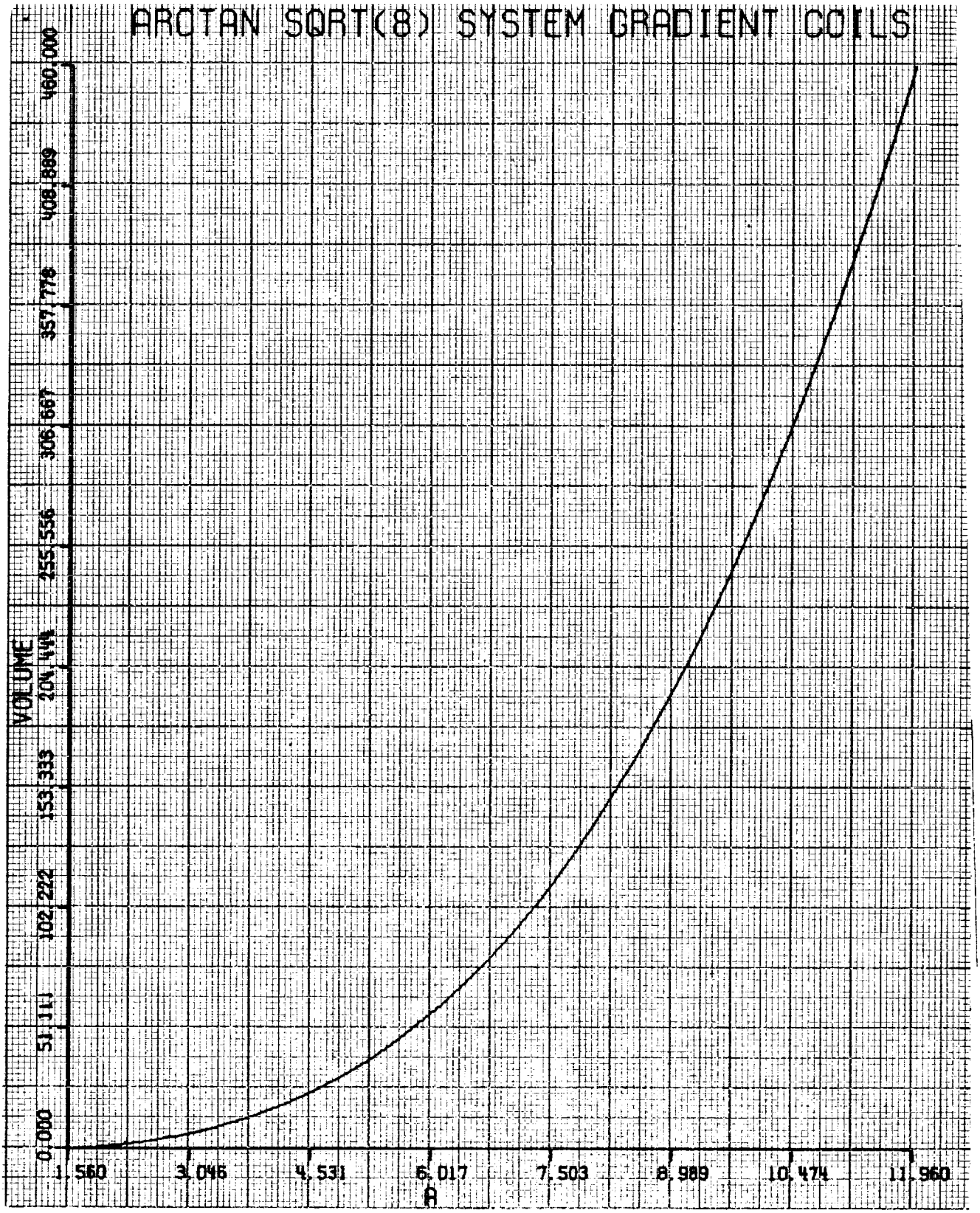
ARCTAN SQRT(8) SYSTEM GRADIENT COILS
VOLUME
0.000
51.111
102.222
153.333
204.444
255.556
306.667
357.778
408.889
460.000
1.560
3.046
4.531
6.017
7.503
8.989
10.474
11.960
A

FIGURE 8

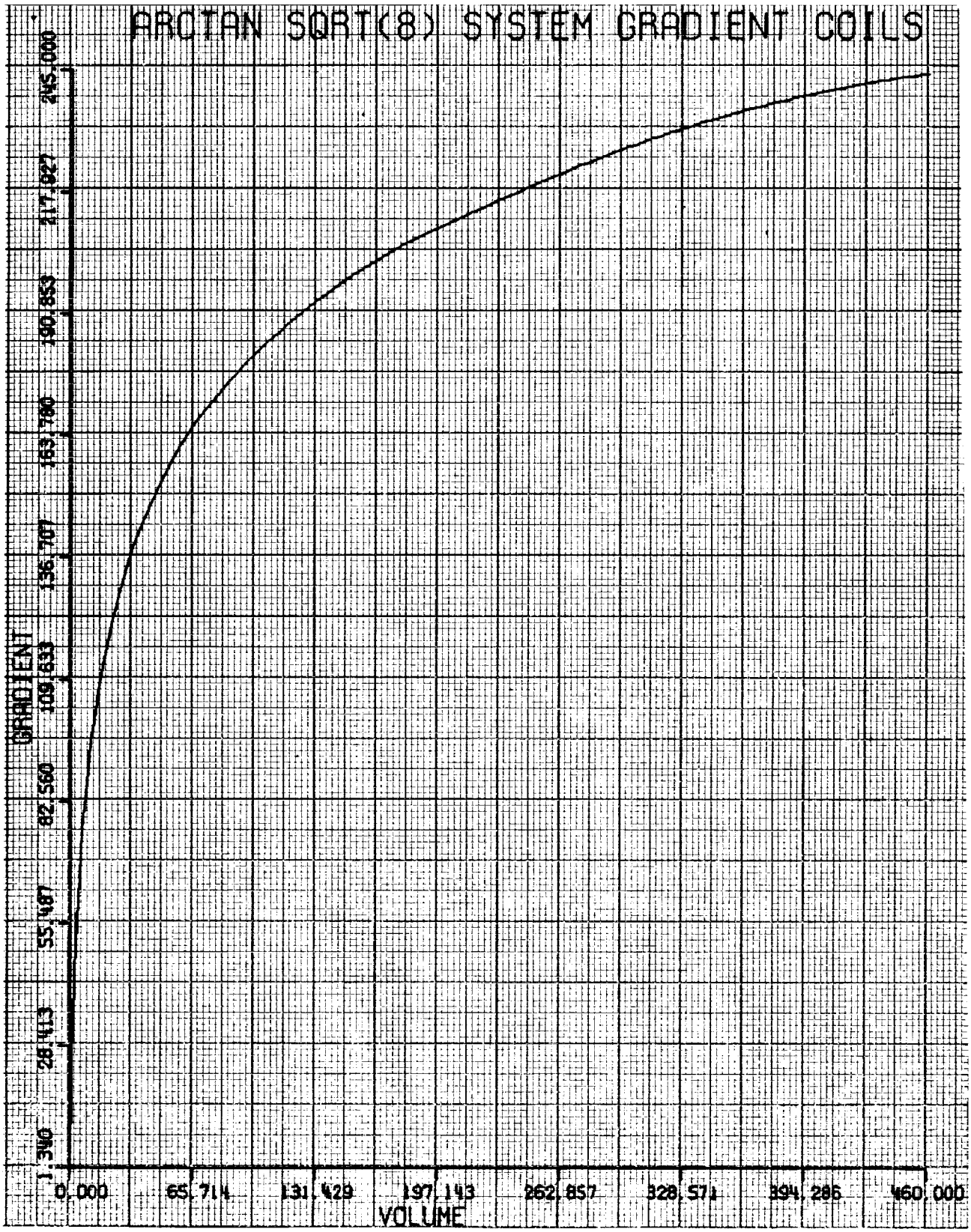
ARCTAN SQRT(8) SYSTEM GRADIENT COILS
GRADIENT
1.390
28.413
55.487
82.560
109.633
136.707
163.780
190.853
217.927
245.000
0.000
65.714
131.429
197.143
262.857
328.571
394.286
460.000
VOLUME

FIGURE 9

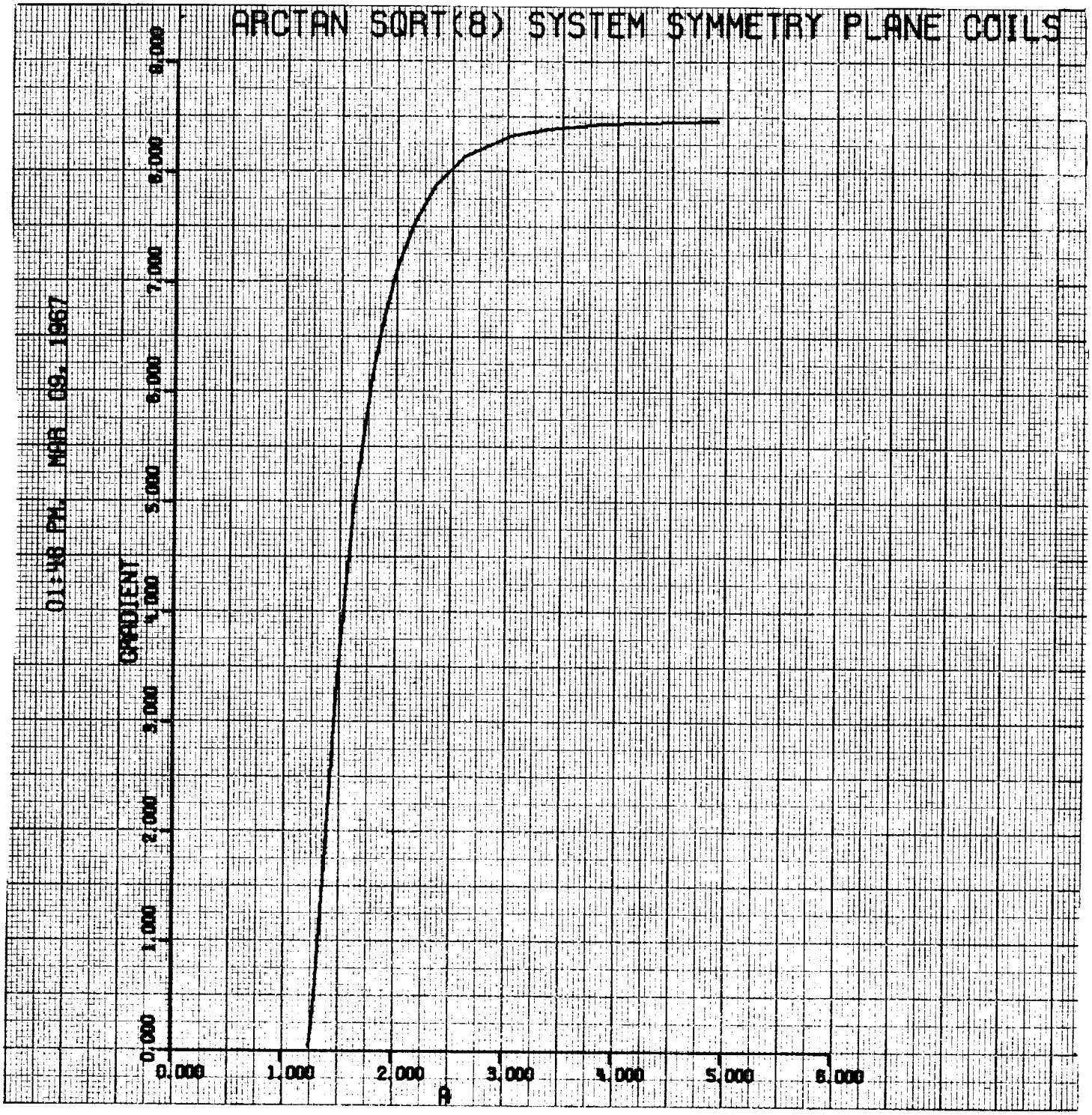
ARCTAN SQRT(8) SYSTEM SYMMETRY PLANE COILS
01:48 PM. MAR 09, 1967
GRADIENT
0.000
1.000
2.000
3.000
4.000
5.000
6.000
7.000
8.000
0.000
1.000
2.000
3.000
4.000
5.000
6.000
R

FIGURE 10

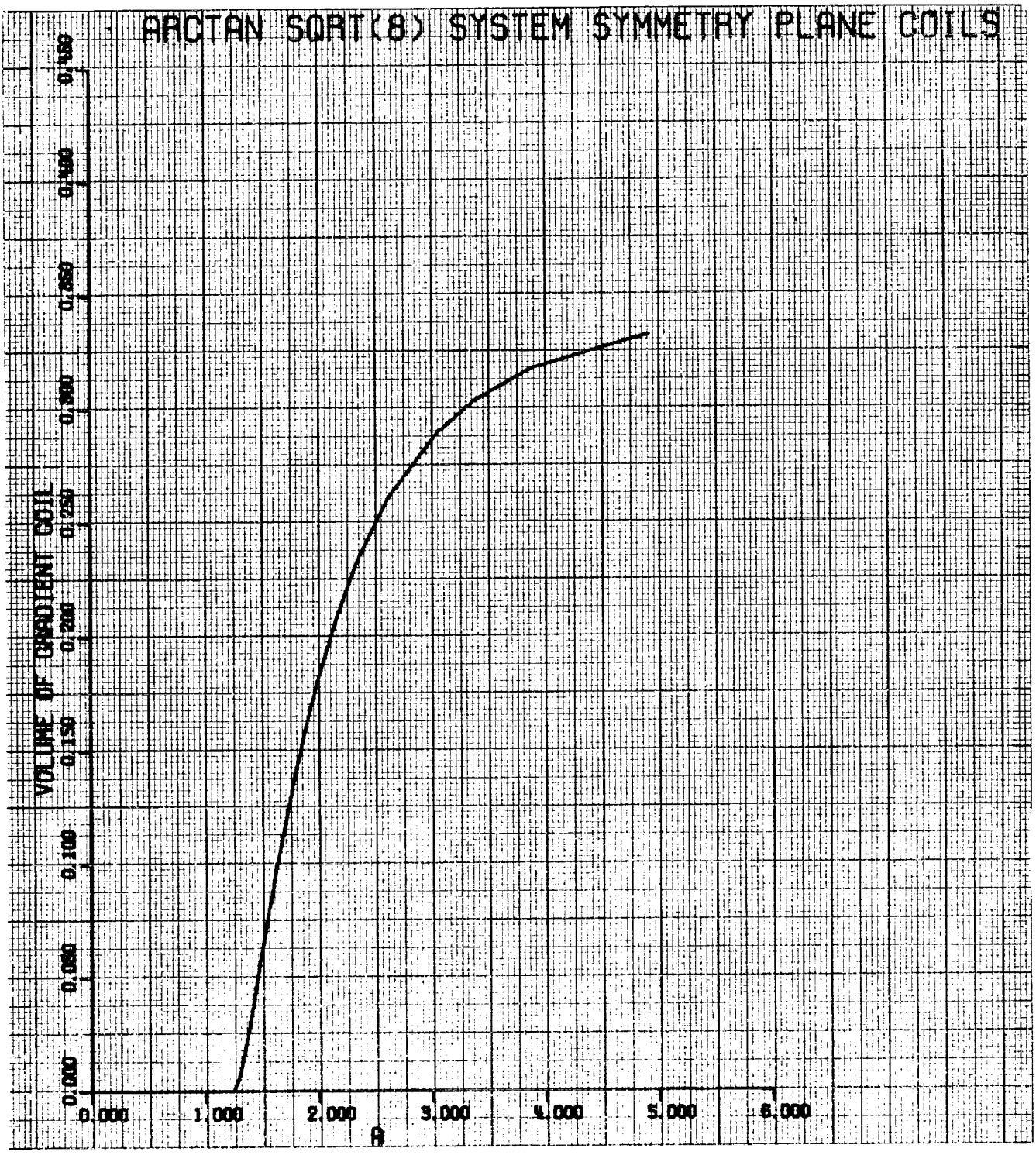
ARCTAN SQRT(8) SYSTEM SYMMETRY PLANE COILS
VOLUME OF GRADIENT COIL
0.000
0.050
0.100
0.150
0.200
0.250
0.300
0.350
0.400
0.450
0.000
1.000
2.000
3.000
4.000
5.000
6.000
R

FIGURE 11

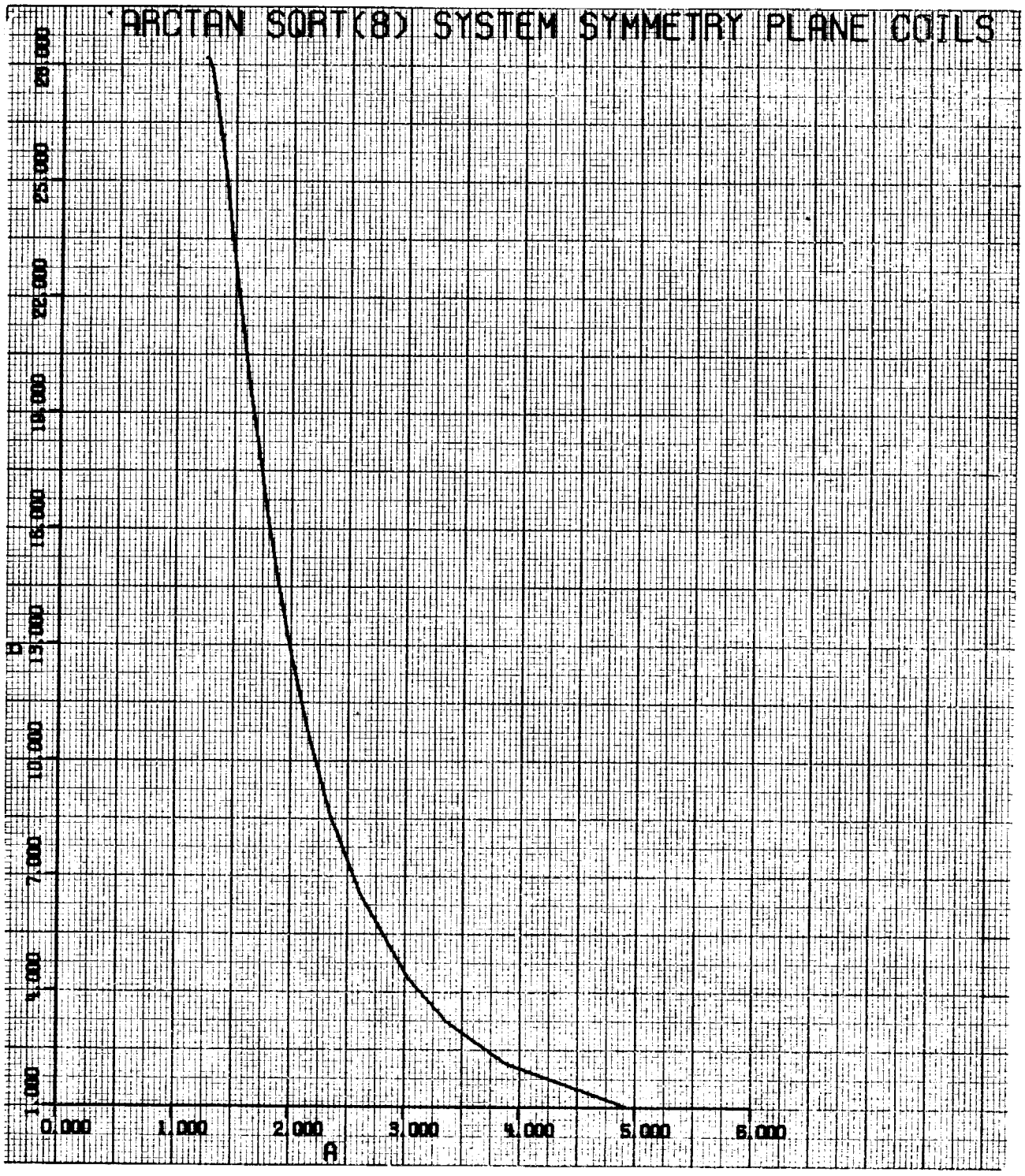
ARCTAN SQRT(8) SYSTEM SYMMETRY PLANE COILS
B
28.000
25.000
22.000
19.000
16.000
13.000
10.000
7.000
4.000
1.000
0.000
1.000
2.000
3.000
4.000
5.000
6.000
A

FIGURE 12

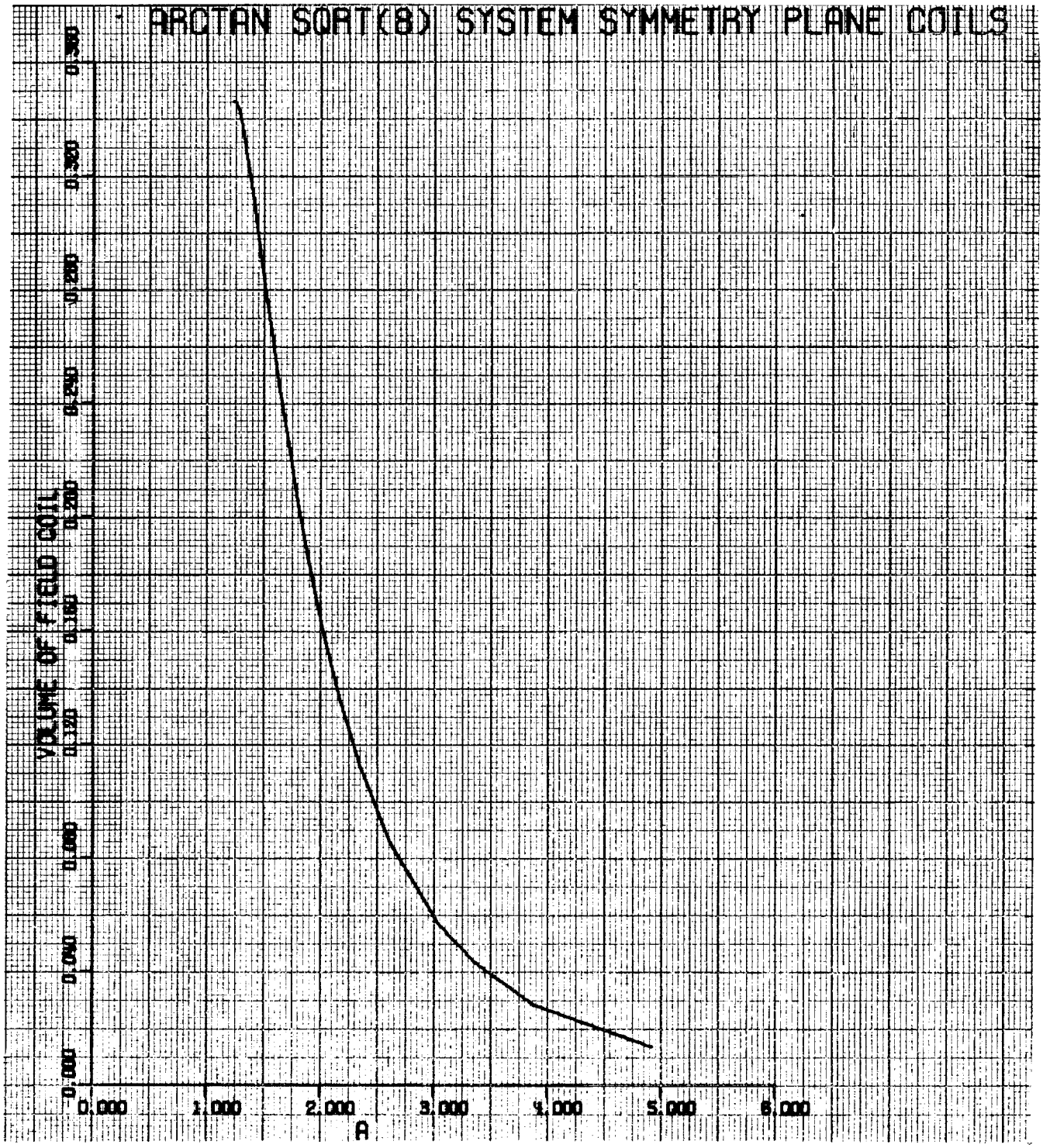
ARCTAN SQRT(8) SYSTEM SYMMETRY PLANE COILS
VOLUME OF FIELD COIL
0.000
0.040
0.080
0.120
0.160
0.200
0.240
0.280
0.320
0.360
0.000
1.000
2.000
3.000
4.000
5.000
6.000
A

FIGURE 13

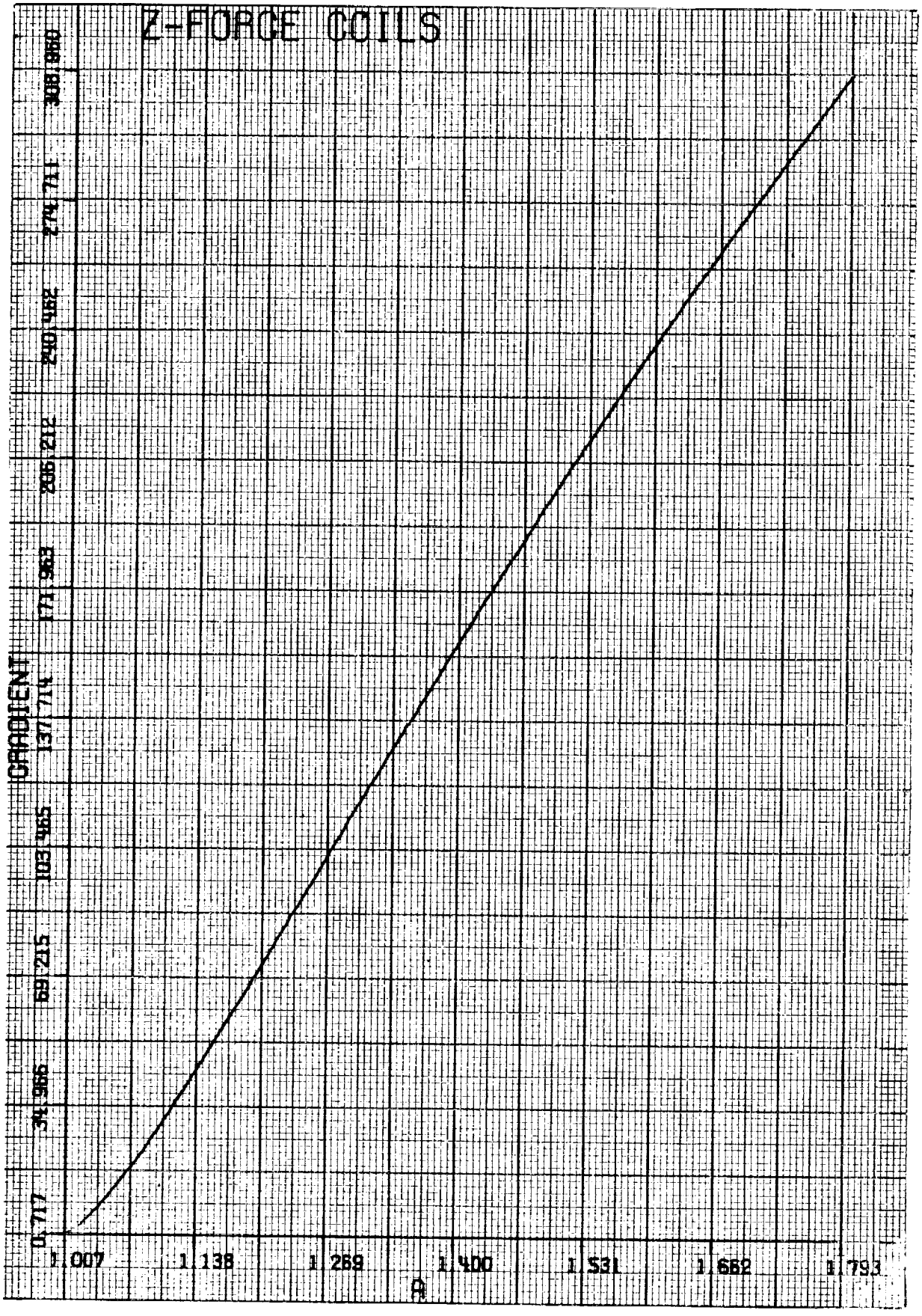
Z-FORCE COILS
CAROUSEL
0.717
34.966
69.215
103.465
137.714
171.963
206.212
240.462
274.711
308.960
1.007
1.138
1.269
1.400
1.531
1.662
1.793
A

FIGURE 14

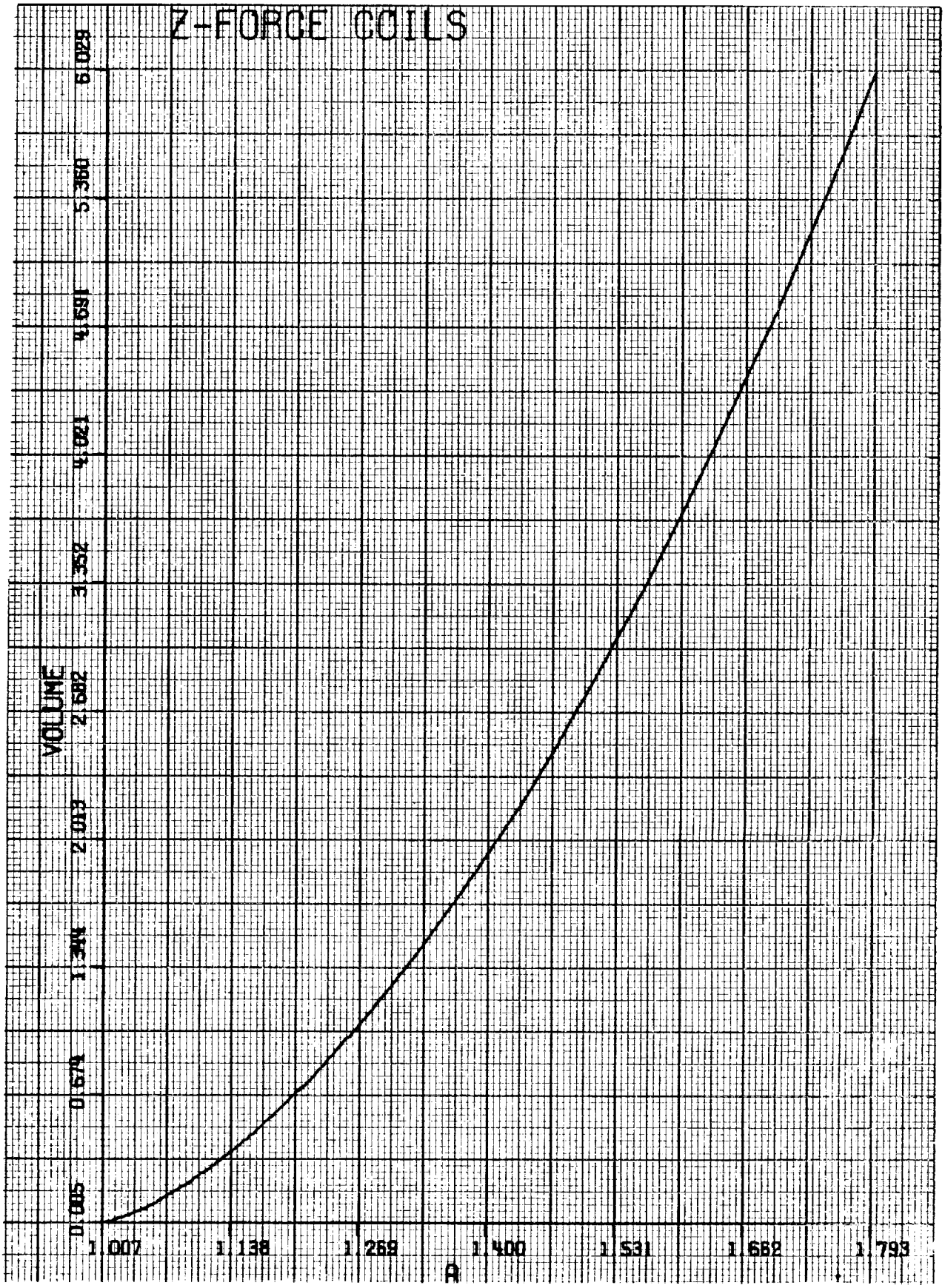
Z-FORCE COILS
VOLUME
0.005
0.670
1.335
2.003
2.682
3.352
4.021
4.691
5.360
6.029
1.007
1.138
1.269
1.400
1.531
1.662
1.793
A

FIGURE 15

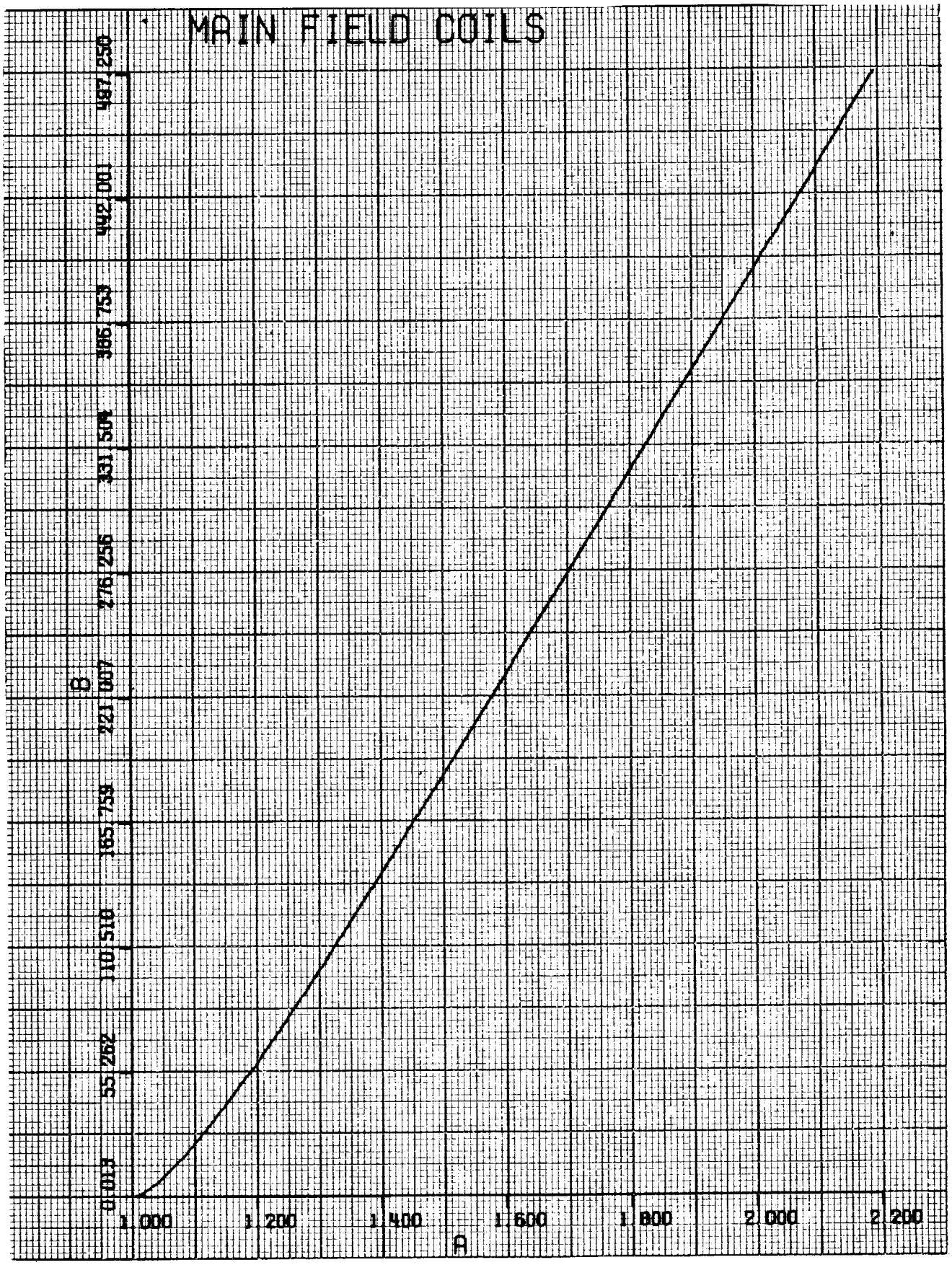
MAIN FIELD COILS
B
A
0
55 262
110 510
165 758
221 007
276 256
331 504
386 753
442 001
497 250
1 000
1 200
1 400
1 600
1 800
2 000
2 200

FIGURE 16

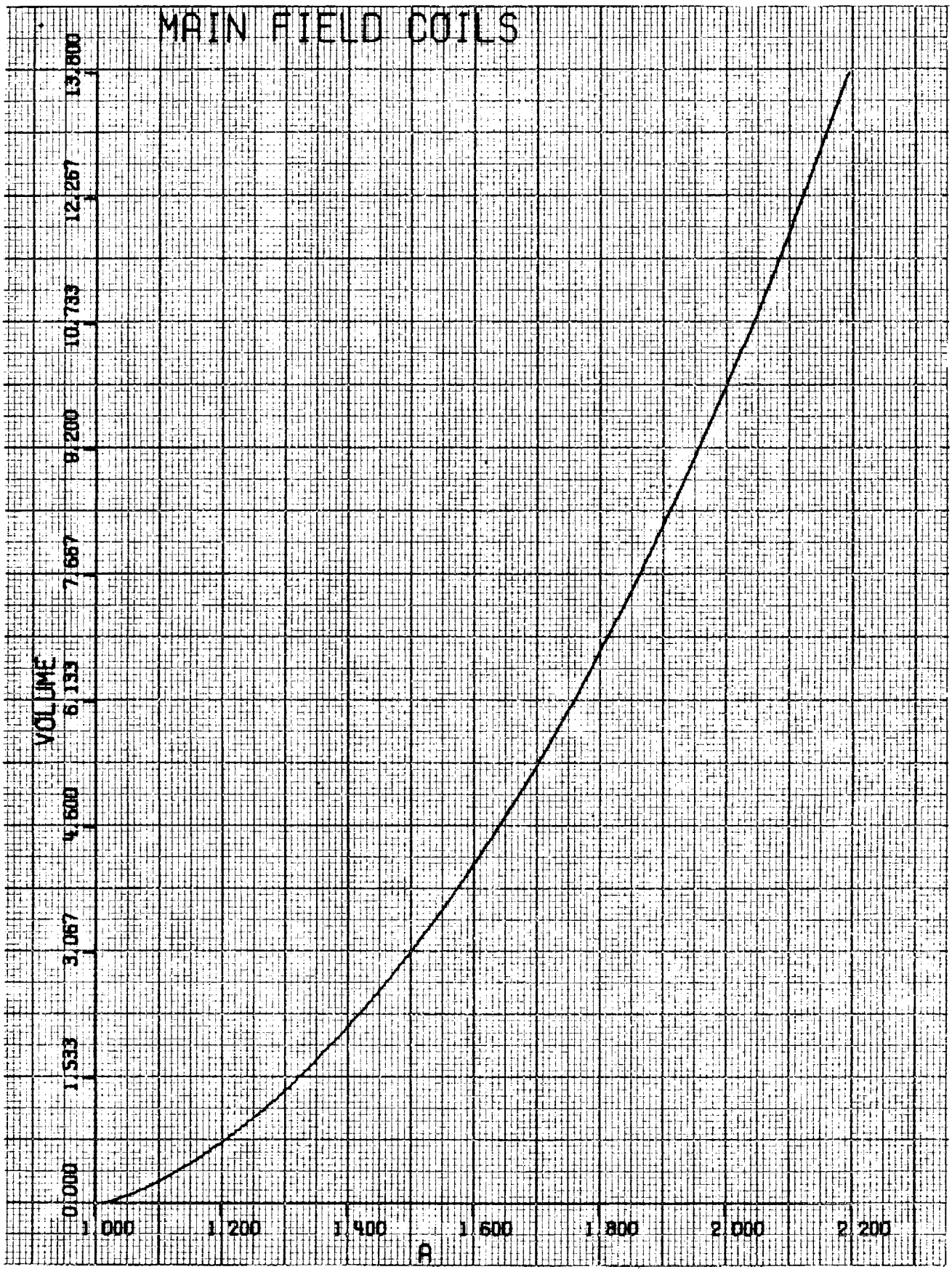
MAIN FIELD COILS
VOLUME
0,000
1,533
3,067
4,600
6,133
7,667
9,200
10,733
12,267
13,800
1 000
1 200
1 400
1 600
1 800
2 000
2 200
A

FIGURE 17

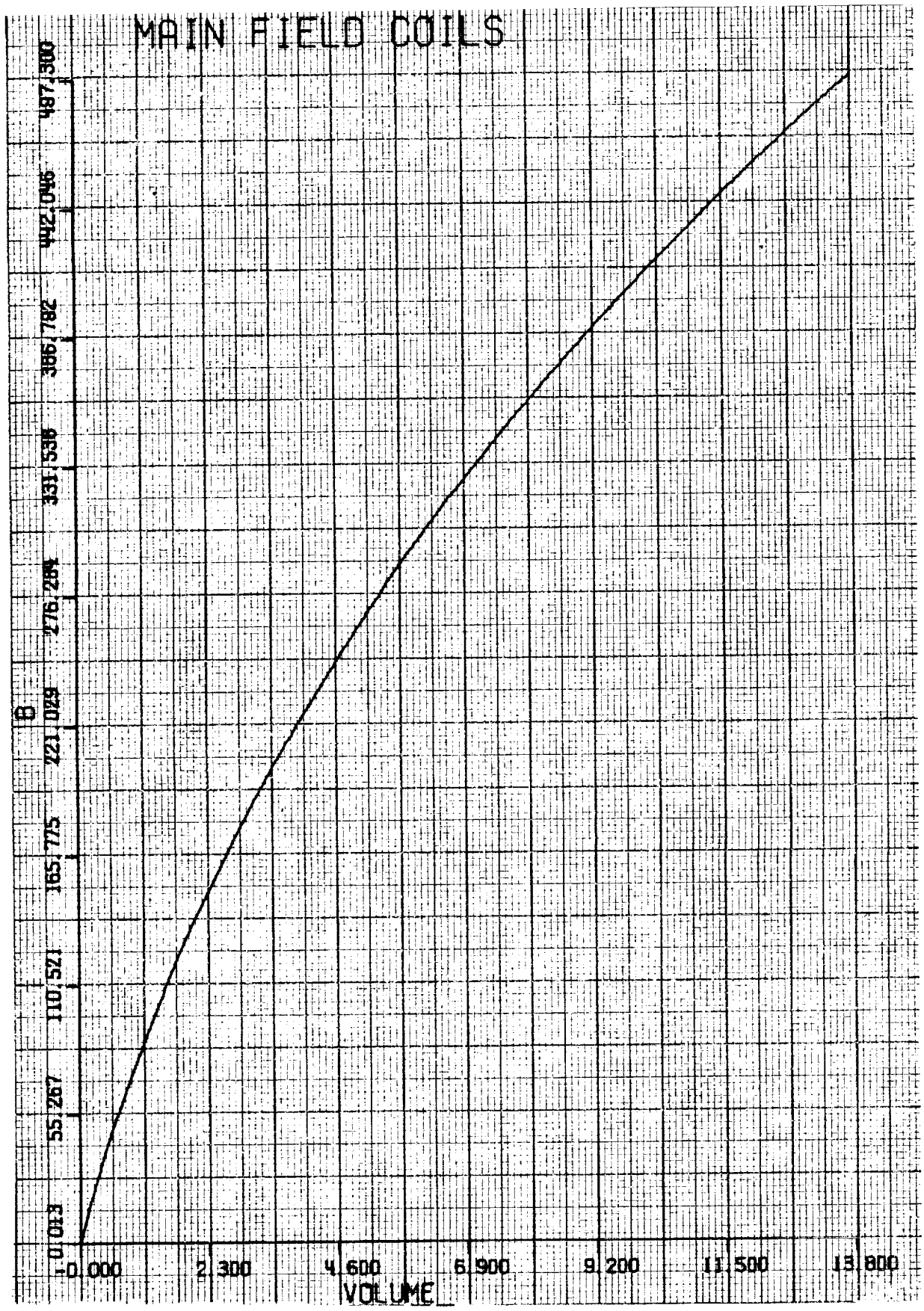
MAIN FIELD COILS
B
0.013
55.267
110.521
165.775
221.029
276.284
331.538
386.782
442.046
497.300
10.000
2.300
4.600
6.900
9.200
11.500
13.800
VOLUME

FIGURE 18

MINIMUM POWER - ARCTAN SQRT(8) SYSTEM
TOTAL POWER - WATTS
0.000
25.000
50.000
75.000
100.000
125.000
150.000
175.000
200.000
0.000
10.000
20.000
30.000
40.000
50.000
60.000
70.000
80.000
90.000
100.000
CURRENT DENSITY - AMP/SQ. CM. x(10⁻⁴)

FIGURE 19

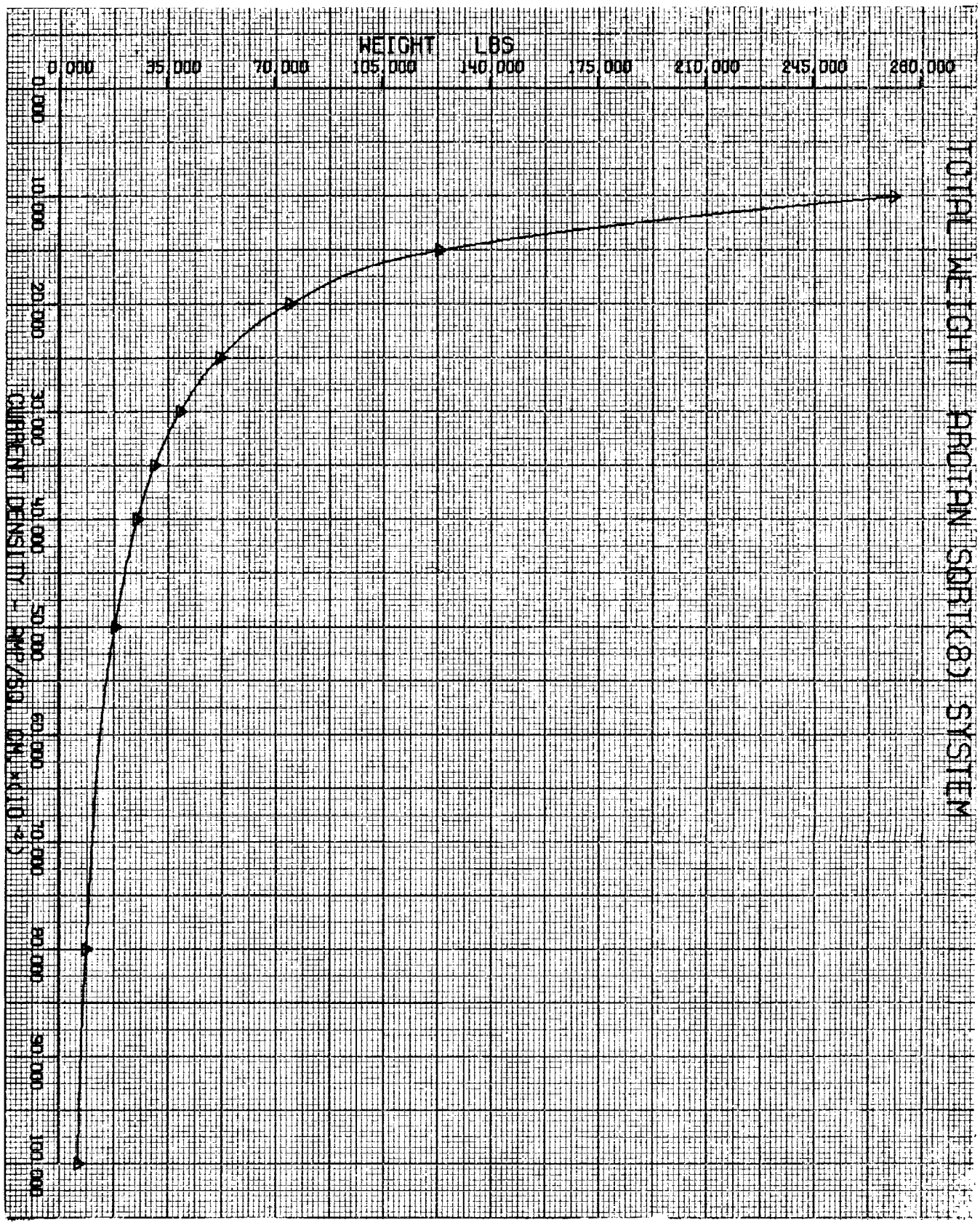
WEIGHT LBS
0 000
35,000
70,000
105,000
140,000
175,000
210,000
245,000
280,000
CURRENT DENSITY, AMPS/SQ. CM. x (10)⁻³
0 000
10 000
20 000
30 000
40 000
50 000
60 000
70 000
80 000
90 000
100 000
TOTAL WEIGHT PROTON SORTC8) SYSTEM

FIGURE 20

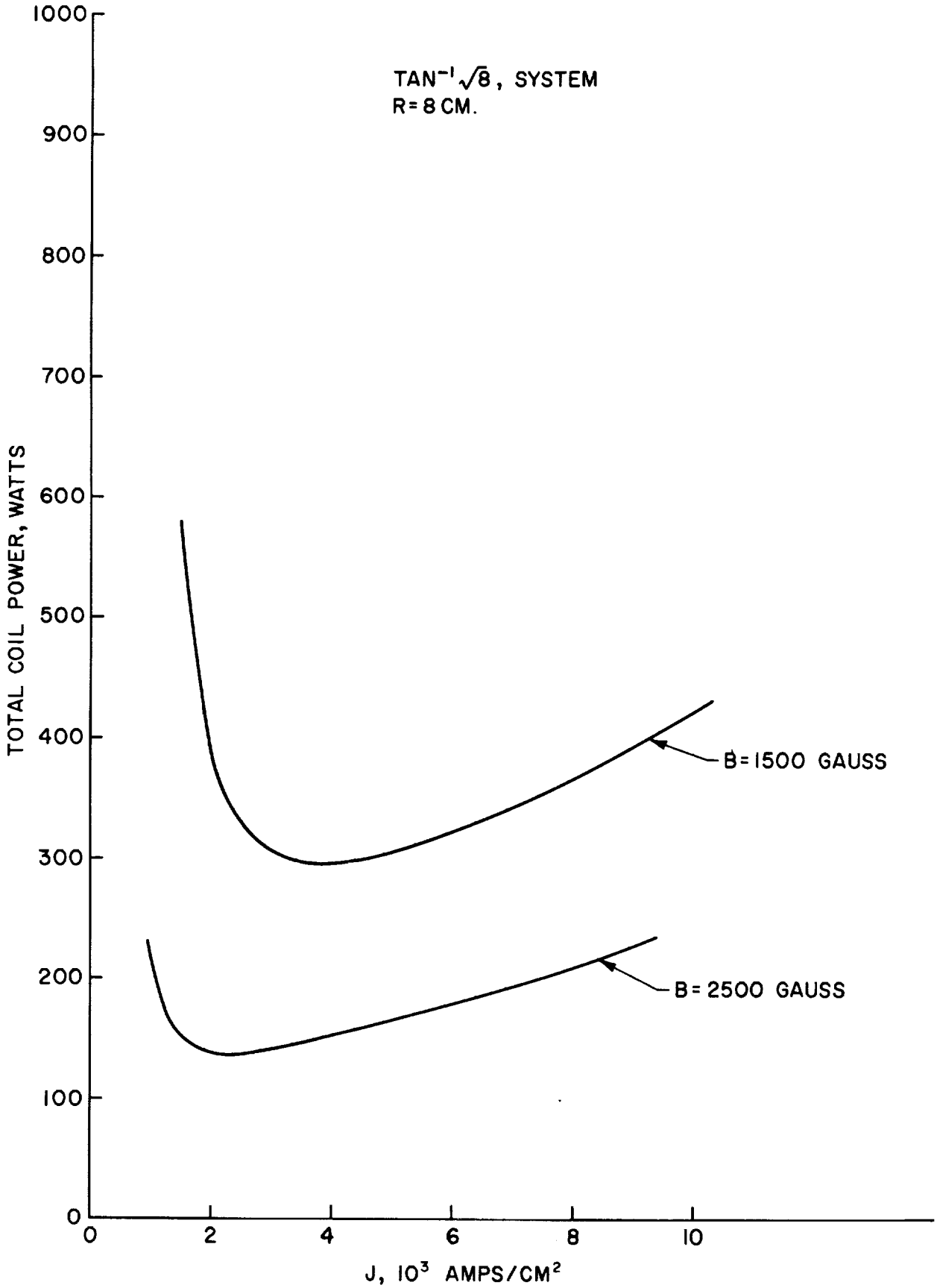
TAN⁻¹√8, SYSTEM
R=8 CM.
TOTAL COIL POWER, WATTS
1000
900
800
700
600
500
400
300
200
100
0
0
2
4
6
8
10
J, 10³ AMPS/CM²
B=1500 GAUSS
B=2500 GAUSS

FIGURE 21

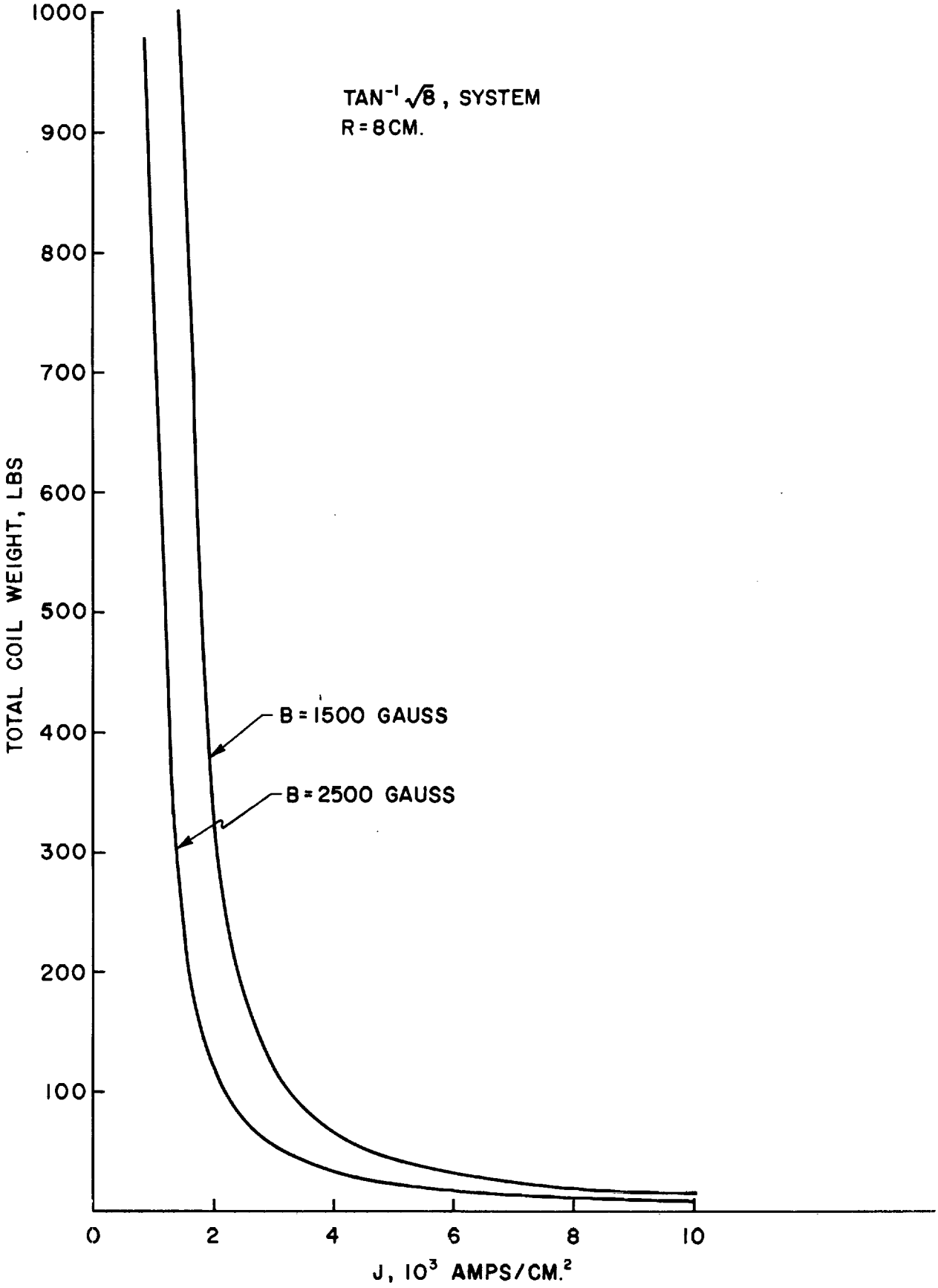
TAN$^{-1}\sqrt{8}$, SYSTEM
R = 8 CM.
B = 1500 GAUSS
B = 2500 GAUSS
TOTAL COIL WEIGHT, LBS
1000
900
800
700
600
500
400
300
200
100
0
2
4
6
8
10
J, 10^3 AMPS/CM.^{2}

FIGURE 22

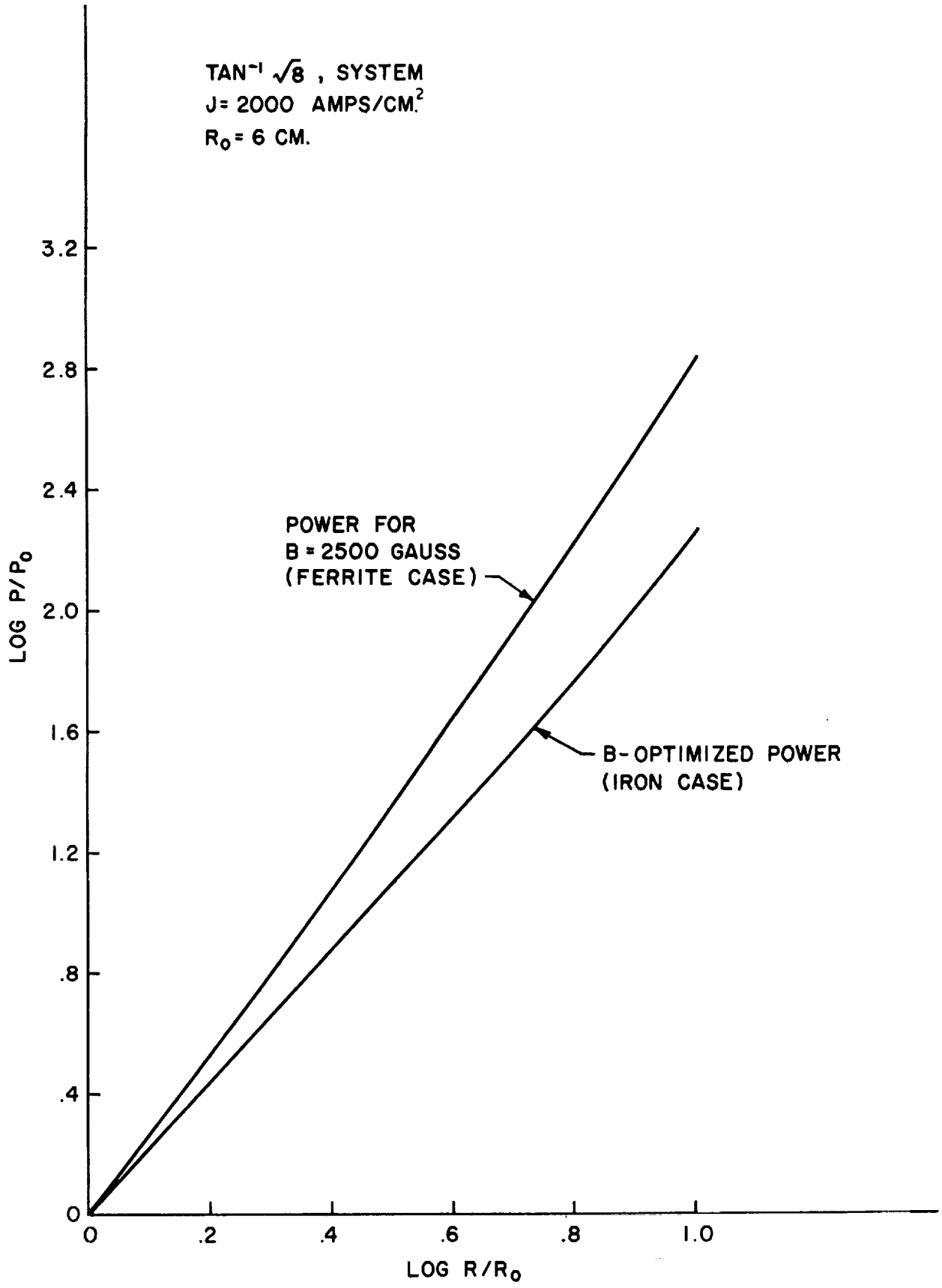
TAN⁻¹ √8 , SYSTEM
J= 2000 AMPS/CM.²
R₀= 6 CM.
3.2
2.8
2.4
2.0
1.6
1.2
.8
.4
0
LOG P/P₀
POWER FOR
B = 2500 GAUSS
(FERRITE CASE)
B-OPTIMIZED POWER
(IRON CASE)
0
.2
.4
.6
.8
1.0
LOG R/R₀

FIGURE 23

DISTRIBUTION LIST

Copy No.	
1 - 10	Grants and Research Contracts Division Office of Space Science and Applications Code SC National Aeronautics and Space Administration Washington, D. C. 20546
11 - 15	Mr. Robert Kilgore Vehicle-Dynamics Section Full-Scale Research Division Langley Research Center, NASA Hampton, Virginia
16 - 18	H. M. Parker
19	A. R. Kuhlthau
20	H. S. Morton
21	R. A. Lowry
22	R. Smoak
23	F. E. Moss
24 - 30	RLES Files
31	Ricardo Zapata